UC San Diego
UC San Diego Previously Published Works

Title
MR Imaging of Atraumatic Muscle Disorders

Permalink
https://escholarship.org/uc/item/0487t4t0

Journal
Radio Graphics, 38(2)

ISSN
0271-5333

Authors
Smitaman, Edward
Flores, Dyan V
Mejía Gómez, Catalina
et al.

Publication Date
2018-03-01

DOI
10.1148/rg.2017170112

Peer reviewed

This copy is for personal use only. To order printed copies, contact **reprints@rsna.org**

1

MUSCULOSKELETAL IMAGING

MR Imaging of Atraumatic Muscle Disorders[1]

Edward Smitaman, MD
Dyan V. Flores, MD
Catalina Mejía Gómez, MD
Mini N. Pathria, MD

SA-CME LEARNING OBJECTIVES

After completing this journal-based SA-CME activity, participants will be able to:

■ Recognize abnormal signal intensity and architectural distortion of muscle at MR imaging.

■ Assign atraumatic muscle disorders to one of four broad MR imaging-based patterns to generate a reasonable differential diagnosis.

■ Recognize key clinical features and MR imaging findings that help narrow the differential diagnosis or suggest a specific diagnosis.

See www.rsna.org/education/search/RG.

Atraumatic disorders of skeletal muscles include congenital variants; inherited myopathies; acquired inflammatory, infectious, or ischemic disorders; neoplastic diseases; and conditions leading to muscle atrophy. These have overlapping appearances at magnetic resonance (MR) imaging and are challenging for the radiologist to differentiate. The authors organize muscle disorders into four MR imaging patterns: *(a)* abnormal anatomy with normal signal intensity, *(b)* edema/inflammation, *(c)* mass, and *(d)* atrophy, highlighting each of their key clinical and imaging findings. Anatomic muscle variants, while common, do not produce signal intensity alterations and therefore are easily overlooked. Muscle edema is the most common pattern but is nonspecific, with a broad differential diagnosis. Autoimmune, paraneoplastic, and drug-induced myositis tend to be symmetric, whereas infection, radiation-induced injury, and myonecrosis are focal asymmetric processes. Architectural distortion in the setting of muscle edema suggests one of these latter processes. Intramuscular masses include primary neoplasms, metastases, and several benign masslike lesions that simulate malignancy. Some lesions, such as lipomas, low-flow vascular malformations, fibromatoses, and subacute hematomas, are distinctive, but many intramuscular masses ultimately require a biopsy for definitive diagnosis. Atrophy is the irreversible end result of any muscle disease of sufficient severity and is the dominant finding in disorders such as the muscular dystrophies, denervation myopathy, and sarcopenia. This imaging-based classification, in correlation with clinical and laboratory data, will aid the radiologist in interpreting MR imaging findings in patients with atraumatic muscle disorders.

©RSNA, 2018 • radiographics.rsna.org

Introduction

Atraumatic skeletal muscle disorders encompass a diverse group of conditions: anatomic variants; congenital, metabolic, acquired, inflammatory, autoimmune, infectious, and ischemic conditions; and benign and malignant masses. Conventional radiography and computed tomography (CT) are useful for detecting intramuscular mineralization, gas, and radiopaque foreign bodies, but they lack the sensitivity for detecting the majority of muscle disorders. Ultrasonography (US) affords high spatial resolution of muscle but is less sensitive than magnetic resonance (MR) imaging for mild edema and early myopathy. US plays an important role in the evaluation of masses, particularly for recognizing muscle variants, distinguishing cystic from solid neoplasms, assessing lesion vascularity, and guiding percutaneous interventions such as aspiration and biopsy. Muscle biopsy can be performed openly or percutaneously, with a greater than 95% success with both methods in obtaining

TEACHING POINTS

- Despite the sensitivity of MR imaging for detecting altered muscle signal intensity and architecture, arriving at a specific diagnosis is often challenging for radiologists, as there is a limited response of muscle to insult, resulting in substantial overlap in the imaging appearances of atraumatic muscle disorders. Correlation with clinical and laboratory findings, other imaging modalities, and, occasionally, tissue sampling is necessary before a diagnosis can be made.

- Accessory muscles are usually asymptomatic and are detected incidentally at imaging, but they may manifest clinically as a painless palpable mass or cause symptoms related to compression of nearby neurovascular structures.

- Edema is the most common pattern of muscle abnormality at MR imaging, appearing as increased signal intensity on T2-weighted or STIR images. T2 mapping affords quantitative assessment of muscle signal intensity and is more sensitive for mild degrees of muscle edema. Correlation with history is especially important in cases of atraumatic muscle edema. Dividing edema into symmetric or asymmetric patterns helps narrow the differential diagnosis: symmetric edema is typical of inflammatory and drug-related myopathies, whereas infection, radiation, myonecrosis, and compartment syndrome tend to be asymmetric and often focal. Additional findings such as architectural distortion of the tissues, intramuscular fluid collections, and extramuscular edema are also helpful.

- Intramuscular masses include malignant or benign primary neoplasms, metastatic disease, and nonneoplastic mass-like lesions related to infection, trauma, inflammation, or other underlying disorders. The differential diagnosis of an intramuscular mass depends on the patient's age, pertinent clinical history, location of the mass, and its imaging appearance. A few intramuscular masses demonstrate unique MR imaging characteristics, allowing a specific diagnosis.

- Atrophy is characterized by loss of muscle tissue that manifests as decreased muscle size, often associated with fatty infiltration. It is the irreversible end stage of numerous muscle diseases, including focal disorders such as trauma or denervation, as well as generalized disorders that are initially inflammatory. Atrophy is the principal finding in hereditary degenerative myopathies that produce disseminated muscle tissue loss without a prodromal inflammatory phase. Atrophy related to aging is referred to as *sarcopenia*, which is increasingly recognized as a substantial predictor of overall health. Atrophy is an important finding predicting loss of muscle power and function.

diagnostic samples. Percutaneous biopsy of muscle disorders can be performed under US or CT guidance using local anesthesia. Open biopsy is more invasive, typically requiring conscious sedation, but the larger tissue samples obtained are more suitable for immunohistochemical analysis and show less sampling error.

MR imaging has emerged as the modality of choice for qualitative assessment of skeletal muscle abnormalities. T1-weighted images show the architecture of the muscle related to its interlaced high-signal-intensity fat, whereas T2-weighted and short-τ inversion-recovery (STIR) images show increased fluid and muscle edema (1,2). Imaging of focal muscle disorders is typically performed using unilateral imaging with a small field of view, but in systemic muscle disorders, large-field-of-view MR imaging (including both sides or whole-body MR imaging techniques) is commonly employed to evaluate symmetry, extent of disease, and response to therapy. A number of novel MR imaging techniques have been employed for the evaluation of muscle disorders, including perfusion and oxygenation mapping; diffusion techniques, including tractography to assess architecture; T2 mapping for quantitative measurement of tissue fluid and fat; MR elastography to evaluate tissue compliance and interstitial fibrosis; and phosphorus (^{31}P) MR spectroscopy to evaluate muscle composition and energetics (3–7).

T2 mapping and MR spectroscopy have been shown to play an important role in the early detection and quantification of muscle dysfunction in a range of disorders, particularly in the assessment of early muscular dystrophies and neuromuscular diseases. While these techniques are currently employed primarily in the research setting, they will play an increasingly important role in muscle imaging.

Normal skeletal muscle is striated and contains interlaced fat within and between major muscle bundles (8) (Fig 1). While muscle tissue itself is hypointense relative to fat and similar to water on T1-weighted images, the overall signal intensity of muscle appears slightly higher than water because of its interspersed fat (Fig 2). Normal muscle is hypointense relative to both fat and water on non–fat-suppressed fluid-sensitive images (9). Despite the sensitivity of MR imaging for detecting altered muscle signal intensity and architecture, arriving at a specific diagnosis is often challenging for radiologists, as there is a limited response of muscle to insult, resulting in substantial overlap in the imaging appearances of atraumatic muscle disorders. Correlation with clinical and laboratory findings, other imaging modalities, and, occasionally, tissue sampling is necessary before a diagnosis can be made.

In this article, we review the typical MR imaging findings of atraumatic muscle disorders, emphasizing the key clinical and imaging findings that will aid radiologists in forming a reasonable differential diagnosis or making the diagnosis when facing abnormal muscle.

Patterns of Muscle Abnormality

Muscle disorders typically manifest as one of four MR imaging patterns: *(a)* abnormal anatomy with normal signal intensity, *(b)* edema/inflammation related to increases in water content, *(c)* intramuscular mass causing anatomic distortion, or *(d)* atrophy resulting in tissue loss, usually accompanied by fatty replacement (10)
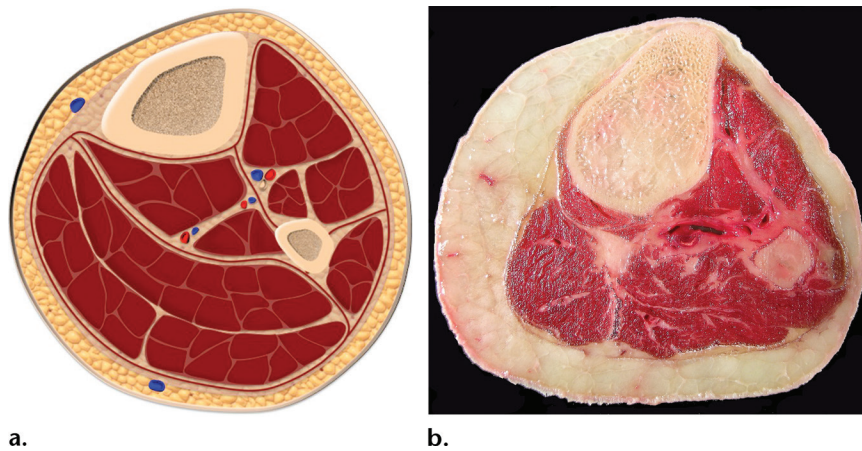
Figure 1. Cross-sectional diagram **(a)** and anatomic photograph of a cross-section specimen **(b)** of the left calf show normal muscle architecture, with its typical feathery or marbled appearance owing to interlaced intramuscular and intermuscular fat. (Specimen courtesy of Donald Resnick, MD, University of California, San Diego, San Diego, Calif.)
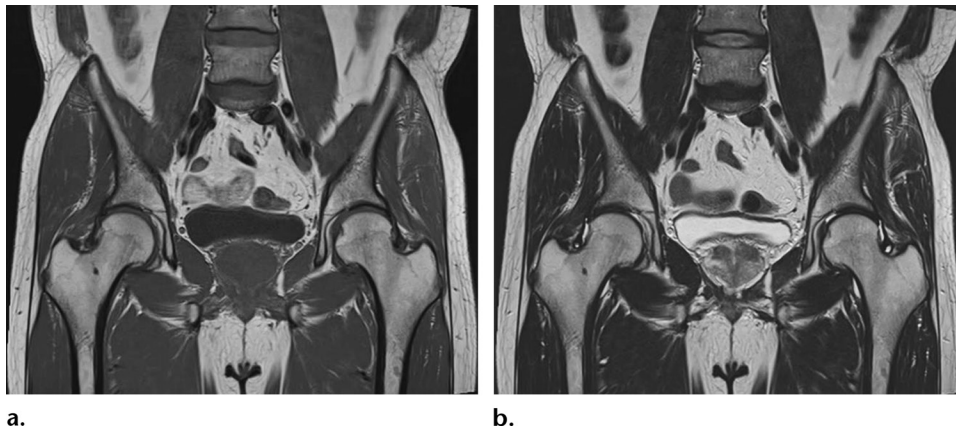

a.

b.

Figure 2. Normal MR images of the muscles of the thigh and pelvis. Coronal T1-weighted **(a)** and T2-weighted **(b)** images show normal pelvic musculature that is symmetric in volume, with smooth convex exterior surfaces that are sharply marginated from the overlying fascia and subcutaneous fat. Interspersed intramuscular and intermuscular fat with high signal intensity is evident on the T1-weighted image **(a)** in a linear or feathery pattern. The signal intensity of muscle remains hypointense on the T2-weighted image **(b)**.

(Table 1). Unfortunately, muscle disorders do not always fit neatly into one of these patterns and instead show a combination of findings such as edema with mass effect (eg, infection with abscess formation) or edema with atrophy (eg, subacute denervation). Other disorders, such as autoimmune myositis, exhibit variable patterns depending on their stage, with edema initially and atrophy after there is irreparable tissue damage. Despite its limitations, we believe this general four-part organizational framework aids interpretation of MR images of atraumatic muscle diseases.

Pattern 1: Abnormal Anatomy with Normal Signal Intensity

Congenital muscle variants include absence of a muscle or muscle group; presence of an accessory (supernumerary) muscle; and deviations of size, course, insertion, or origin of a normally present (anomalous) muscle (11). Muscle herniation, which can be caused by congenital or posttrau-

matic fascial weakening, and surgical procedures altering myotendinous anatomy can also produce a similar pattern of architectural abnormality without signal intensity alterations (Fig 3). Recognition of anatomic variations can be challenging at MR imaging unless one is thoroughly familiar with normal regional anatomy. Fiducial markers are helpful for identifying this category of muscle abnormalities. Congenital absence of a small extremity muscle is often asymptomatic, whereas absence of a critical muscle involved in fine motor control (eg, ocular muscle) or a large muscle (eg, pectoralis) may result in dysfunction or deformity, respectively. In cases of accessory and anomalous muscles, T1-weighted images best depict the muscular architecture of the "lesion," while T2-weighted images are useful to help confirm muscle signal intensity.

Accessory Muscle

An accessory muscle is the most common form of congenital muscle variation, seen in 1%–5%

Table 1: Patterns of Nontraumatic Muscle Disorders at MR Imaging

Abnormal anatomy
  Absent muscle
  Accessory muscle
  Anomalous muscle
  Muscle hernia
  Postoperative

Edema and inflammation
  Inflammatory myositis
  Drug-related myopathy
  Human immunodeficiency virus
    (HIV)–related myopathy
  Muscle infection
  Radiation
  Myonecrosis

Intramuscular mass
  Primary neoplasm
  Metastatic disease
  Hematoma
  Nodular myositis
  Sarcoidosis
  Postinjection
  Crystal deposition

Muscle atrophy
  End stage of inflammation
  Congenital myopathy
  Denervation myopathy
  Sarcopenia

Figure 3. Muscle flap. Axial T1-weighted MR image of the left calf shows anatomic distortion of the anterior leg, with muscle tissue overlying the anteromedial surface of the tibia (arrows), related to a surgical musculocutaneous flap constructed for a chronic ulcer. Note that the signal intensity and architecture of the anteriorly transposed gastrocnemius muscle remain normal.

Figure 4. Accessory soleus muscle in a middle-aged man with atraumatic posterior ankle soreness and soft-tissue fullness. Sagittal midline T1-weighted MR image of the right ankle shows a large accessory soleus muscle (∗) within the pre-Achilles fat pad, inserting onto the upper calcaneus. There are linear regions of internal fat within it, and its signal intensity characteristics are identical to those of normal muscle.

of individuals, typically involving the hands and feet (11,12). Accessory muscles are usually asymptomatic and are detected incidentally at imaging, but they may manifest clinically as a painless palpable mass or cause symptoms related to compression of nearby neurovascular structures. The extensor digitorum brevis manus muscle, located dorsally at the level of the carpometacarpal joint, typically arises from the dorsal wrist capsule and inserts on the index or middle finger (11). It commonly manifests as a painless mass overlying the carpus, often mistaken clinically for a ganglion cyst or carpal boss (13).

The accessory soleus muscle also commonly manifests as a mass, typically in adolescents or young adults, possibly related to increased muscle mass and physical activity at these ages (14). It arises from the fibula, soleal line of the tibia, or anterior soleus muscle and traverses through the pre-Achilles fat pad to insert on the superior or medial calcaneus (15) (Fig 4). Accessory muscles can lead to nerve compression when they overlie a nerve within a fibro-osseous tunnel. Compression of the ulnar nerve at the cubital tunnel by an accessory anconeus epitrochlearis muscle, the median or ulnar nerves at the wrist by palmar ac-
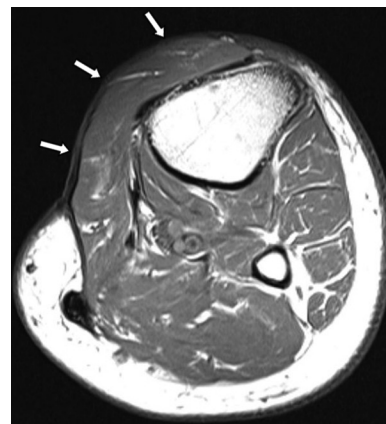
cessory muscles, and the tibial nerve by an accessory flexor muscle at the tarsal tunnel are all well recognized (11,15) (Fig 5).

Anomalous Muscle
Numerous anomalies of the course, insertion, or origin of muscles have been described. The majority are asymptomatic, but they can occasionally result in clinical symptoms, similar to those of accessory muscles. Anomalous muscles from
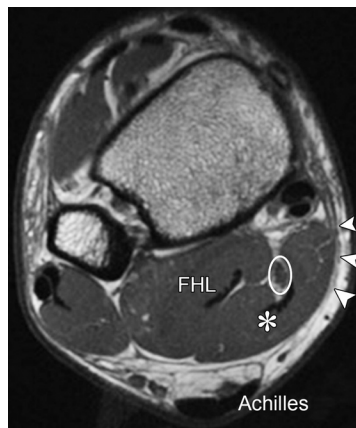
RadioGraphics

Figure 5. Accessory muscle in a 28-year-old woman with right ankle discomfort. Axial T1-weighted MR image of the right ankle shows an accessory tibiocalcaneus internus muscle (∗) in its characteristic location: posterior to the flexor hallucis longus muscle *(FHL)*, superficial to the tibial neurovascular bundle (oval), and deep to the flexor retinaculum (arrowheads). This uncommon accessory muscle originates from the medial crest of the tibia and courses superficially to the tibial nerve at the tarsal tunnel to insert at the medial calcaneus, a few centimeters anterior to the Achilles tendon.
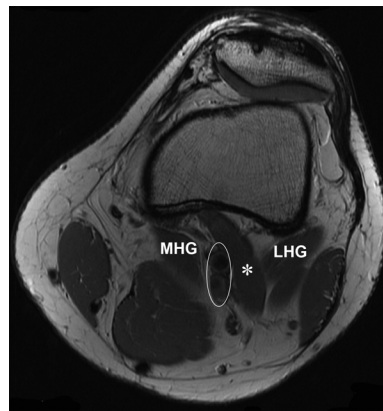

Figure 6. Third head of the gastrocnemius muscle causing popliteal artery entrapment in a 32-year-old man with long-standing lower extremity pain on exertion. Axial proton density (PD)–weighted MR image of the left knee shows an anomalous muscle slip (∗) arising from the lateral head of the gastrocnemius muscle *(LHG)*, extending medially, and coursing laterally and anteriorly to the popliteal vascular bundle (oval). A US image (not shown) of the left popliteal artery showed decreased arterial flow during plantar flexion against resistance. *MHG* = medial head of the gastrocnemius muscle.

the forearm or palm extending into the carpal tunnel can cause median nerve compression. An anomalous plantaris insertion on the lateral patellar retinaculum can cause iliotibial band syndrome or result in patellar maltracking (16). The medial and lateral gastrocnemius muscles may have anomalous insertions that can cause popliteal artery entrapment, manifesting as diminished pulses with ankle movement or intermittent claudication with exertion (11) (Fig 6).

Pattern 2: Edema/Inflammation

Edema is the most common pattern of muscle abnormality at MR imaging, appearing as increased signal intensity on T2-weighted or STIR images. T2 mapping affords quantitative assessment of muscle signal intensity and is more sensitive for mild degrees of muscle edema (Fig 7). Correlation with history is especially important in cases of atraumatic muscle edema.

Dividing edema into symmetric or asymmetric patterns helps narrow the differential diagnosis: symmetric edema is typical of inflammatory and drug-related myopathies, whereas infection, radiation, myonecrosis, and compartment syndrome tend to be asymmetric and often focal (Table 2). Additional findings such as architectural distortion of the tissues, intramuscular fluid collections, and extramuscular edema are

also helpful (1). While it is difficult to establish a specific diagnosis in many cases of muscle edema, MR imaging is still helpful for localizing active disease to guide biopsy (2,9,17).

Idiopathic Inflammatory Myositis

The idiopathic inflammatory myopathies are a group of chronic autoimmune disorders that result in muscle weakness and inflammation, primarily affecting proximal extremity muscles. These disorders have overlapping clinical and imaging features, and the diagnostic criteria and classification systems are continually evolving (18,19). The original classification proposed by Bohan et al (20) divided inflammatory myopathies into five types: *(a)* adult dermatomyositis, *(b)* adult polymyositis, *(c)* juvenile myositis, *(d)* myositis associated with cancer, and *(e)* myositis associated with connective tissue disease (overlap syndrome). Subsequently, other forms of autoimmune myositis, such as necrotizing autoimmune myopathy and inclusion body myositis, have been included (18). Current classification systems no longer distinguish between the adult and juvenile forms of these disorders (18).

Polymyositis and Dermatomyositis.—The best-known inflammatory myopathies are polymyositis and dermatomyositis. Both initially involve the proximal lower limb muscles, particularly the hamstrings, before ascending to involve the buttocks,
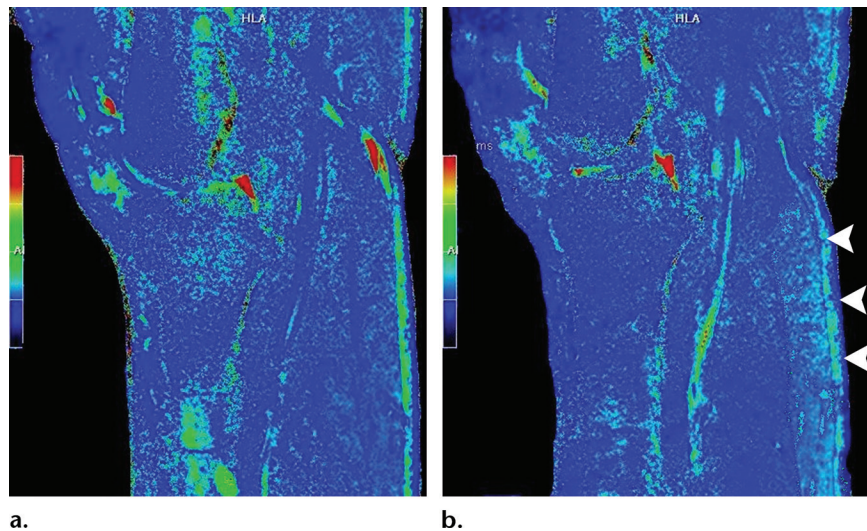
Figure 7. T2 mapping in a 54-year-old man with pain after exercise. Sagittal resting **(a)** and postexercise **(b)** T2 maps of the calf show mild T2 prolongation in the medial head of the gastrocnemius muscle (arrowheads in **b**) (25 msec at rest, compared with 40 msec after exercise), indicating increased extracellular fluid owing to ischemia. This is a nonspecific finding that can be seen related to postexercise ischemia from chronic exertional compartment syndrome or perfusion abnormalities.

proximal upper limbs, neck flexors, and pharyngeal muscles (18,21). MR imaging shows symmetric edema with preserved muscle architecture, typically associated with considerable subcutaneous and perifascial thickening and fluid (21,22). Muscle edema can be patchy, inhomogeneous, and variegated, even within an individual muscle (1,21) (Fig 8).

In dermatomyositis, amorphous or sheetlike muscle and fascial calcifications may also manifest and are often difficult to appreciate at MR imaging. Edema correlates roughly with disease activity and may resolve with anti-inflammatory medications (22). At the chronic/burned-out stage, MR imaging shows nonspecific patchy symmetric muscle atrophy without inflammation (Fig 9). Whole-body MR imaging can potentially help assess disease burden and activity and reveal atypically involved sites, such as distal muscles (21).

Paraneoplastic Myositis.—Although controversial, an association between inflammatory myopathies and malignancy has been described. In some series, up to 24% of patients presenting with polymyositis or dermatomyositis either have or are subsequently diagnosed with a malignancy, typically within 1–2 years following myositis onset (19,23). Associated malignancies include lung, genitourinary, and gastrointestinal carcinomas and non-Hodgkin lymphomas (19,23). In some patients, an increase in inflammatory symptoms heralds recurrent malignancy, suggesting that myositis reflects an immune response against neoplastic cells (19).

Overlap with Connective Tissue Disease.—Autoimmune connective tissue disorders such as scleroderma, systemic lupus erythematosus (SLE), Sjögren syndrome, rheumatoid arthritis, mixed connective tissue disease, and overlap syndromes can be complicated by inflammatory myopathy (24,25). Muscle involvement is most common in scleroderma or in an overlap syndrome that includes scleroderma, affecting 5%–96% of such patients, portending a poor prognosis. Up to 28% of patients with rheumatoid arthritis or SLE demonstrate myositis with muscle necrosis and inflammation of connective tissues (25–27). At MR imaging, the myositis related to collagen vascular disorders is indistinguishable from polymyositis (25).

Inclusion Body Myositis.—Inclusion body myositis is a common myopathy in older patients that is diagnosed histologically by distinct inclusion bodies in the nuclei and cytoplasms of affected muscle cells. It develops insidiously, often without substantially elevated inflammatory markers and muscle enzymes. Unlike conventional inflammatory myositis, inclusion body myositis can be asymmetric and often affects the pharyngeal muscles, upper extremities, and distal musculature early in the course of the disease (18). The dominant finding is prominent patchy muscle atrophy without substantial inflammation or perifascial edema (2,9) (Fig 10).

Drug-related Myopathy

Muscle can be exposed to drugs systemically or directly through inoculation, resulting in diffuse

Table 2: Muscle Edema (Increased T2 Signal Intensity): Differential Diagnosis

Muscle Disorder	Clinical Findings	Distribution	T1-weighted Findings	T2-weighted Findings	Tissue Architecture	Adjacent Soft Tissues	Enhancement after Contrast Medium Administration
Bilateral, symmetric, and multiple muscles							
Polymyositis	Proximal muscle weakness	Proximal lower limbs	Normal	Edema	Normal	Edema	Mild
Dermatomyositis	Skin rash	Proximal lower limbs	Normal	Edema	Normal	Edema and/or calcification	Mild
Drug-related myopathy	Temporal link with drug usage	Proximal lower limbs	Normal	Edema	Normal	Edema	Variable
HIV-related myopathy	HIV positive	Proximal lower limbs	Normal	Edema	Normal	Edema	Variable
Inclusion body myositis	Older patients	Quadriceps, upper extremities	Normal	Mild edema	Normal	Normal	Variable
Unilateral/focal with normal architecture							
Radiation	Radiation history	Dependent on the site of the radiation portal	Normal	Bandlike demarcation from nonirradiated tissue	Normal	Operative changes may manifest	Variable
Denervation	Neuropathy	Follows a nerve distribution	Normal (acute) or atrophy (subacute and chronic)	Mild uniform edema (acute and subacute)	Normal	Normal	No enhancement
Unilateral/focal with abnormal architecture							
Pyomyositis	Can be multifocal, if immunocompromised	Thighs	High-signal-intensity rim with abscesses	Edema	Fluid collections	Extensive edema	Rim enhancement of abscesses
Acute compartment syndrome (ACS)	Surgical emergency	Lower leg	Mild hyperintensity	Edema	Normal	Mild edema	Nonenhancement of necrotic areas
Chronic compartment syndrome	Can manifest as a mass	Lower leg	Low-signal-intensity calcifications	Central fluid collection	Peripherally calcified mass	Variable	Nonenhancement of necrotic areas
Diabetic myonecrosis	Poorly controlled diabetes	Anterior thigh or calf; can be multifocal	Enlarged and effaced tissue; occasional hemorrhage	Edema	Fluid collections	Perifascial edema	Nonenhancement of necrotic areas

a.

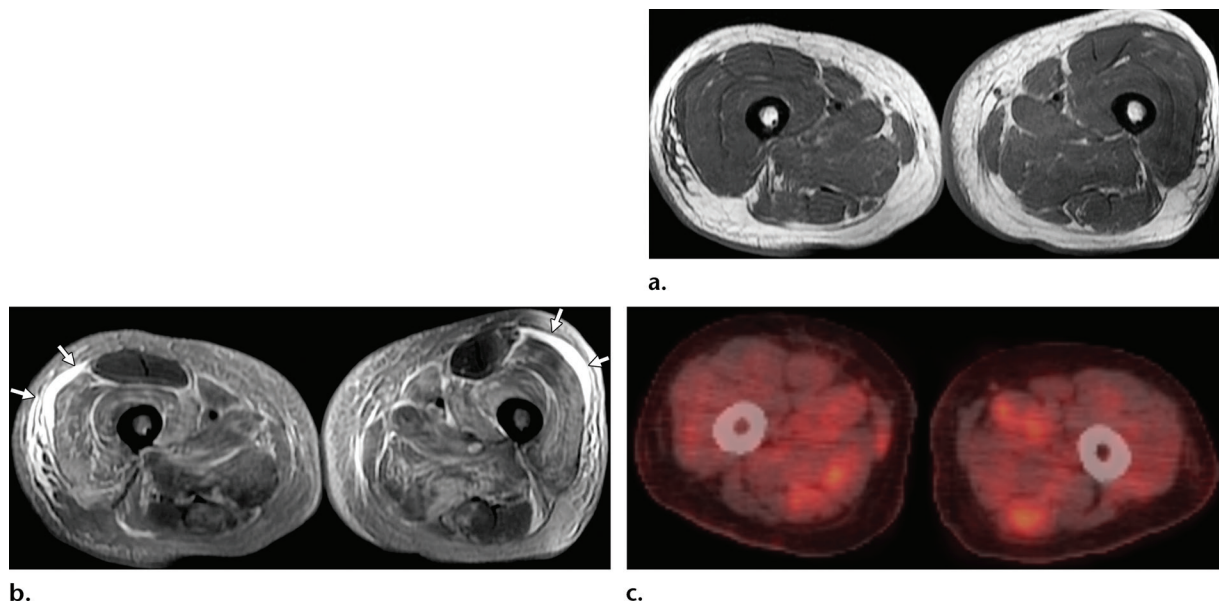b.   c.

Figure 8. Dermatomyositis in a 50-year-old man with bilateral lower extremity weakness. **(a)** Axial T1-weighted MR image shows no substantial distortion of the muscle architecture. **(b)** Axial fat-suppressed T2-weighted MR image shows relatively symmetric muscle edema, with subcutaneous and perifascial fluid (arrows) in both thighs. There is involvement of multiple muscle compartments, but it is patchy, with relative sparing of the rectus femoris and portions of the hamstring musculature. **(c)** Axial fluorine 18 fluorodeoxy-glucose (FDG)–positron emission tomography (PET)/CT image shows matching increased activity in the inflamed musculature. The results of a muscle biopsy disclosed dermatomyositis.
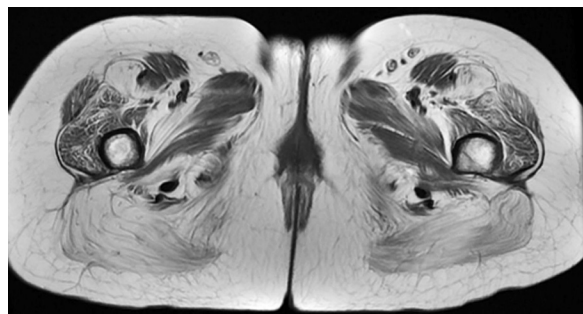

Figure 9. Symmetric patchy atrophy in a 55-year-old woman with a long-standing history of inflammatory myositis, currently in remission. The patient had been variably diagnosed with either polymyositis or myositis associated with connective tissue disorder. Axial T1-weighted MR image of the proximal thighs shows bilateral symmetric atrophy of the pelvic and thigh musculature. The atrophy is somewhat patchy, most prominently at the gluteus maximus, vastus lateralis, and lateral portion of the rectus femoris muscles, with relative sparing of the adductor muscles. Symmetric patchy atrophy is a common sequela of all forms of long-standing inflammatory myositis.
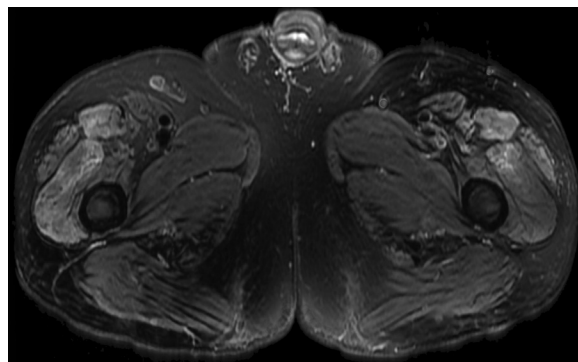

Figure 10. Inclusion body myositis in a 71-year-old man who presented with slowly progressive bilateral leg weakness. Axial fat-suppressed T2-weighted MR image of both thighs shows symmetric increased signal intensity in the quadriceps muscles bilaterally. There is no substantial associated muscle atrophy or subcutaneous edema. The results of a subsequent muscle biopsy showed scattered subsarcolemmal vacuoles with blue granular rims, findings typical of inclusion body myositis.

or local tissue damage, respectively. Dysfunction related to systemic drug administration affects multiple muscles bilaterally, causing muscle weakness, myopathy, inflammation, and, in extreme cases, rhabdomyolysis.

Imaging findings are nonspecific, consisting of symmetric increased muscle size and edema, typically affecting the buttocks, quadriceps, adductors, and deep calf muscles (28). The most common drugs associated with myopathy are the HMG-CoA reductase inhibitors (statins), used for treating dyslipidemia. Statin-induced

muscle pain and weakness develop in up to 5% of treated patients (28). This mild form, referred to as *toxic statin myopathy*, is dose dependent and resolves with cessation of the drug. A small subgroup, approximately one in 10 000 patients treated with statins, develop a severe myositis that may persist or progress even after discontinuation of the drug. This form, known as *autoimmune necrotizing myopathy*, can progress to rhabdomyolysis and requires immunosuppressive therapy (29,30). Substantial creatine kinase level elevation and autoantibodies directed
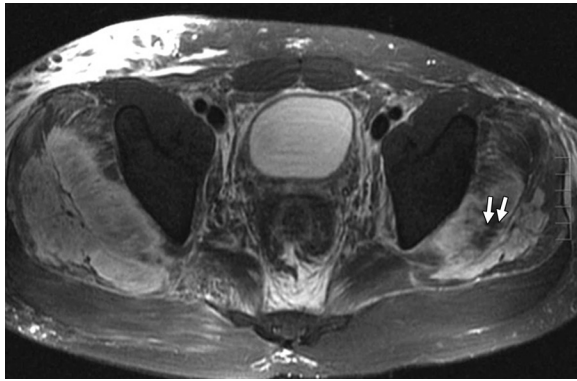
Figure 11. Rhabdomyolysis in a 22-year-old man with a history of cocaine use who presented with bilateral hip pain and elevated creatine kinase levels after a prolonged cocaine binge. Axial fat-suppressed T2-weighted MR image of the pelvis shows patchy regions of increased signal intensity in the gluteal minimus and medius muscles bilaterally, the right worse than the left, related to myonecrosis. Note the stippled appearance of residual intact muscle fibers in the left gluteal musculature (arrows).
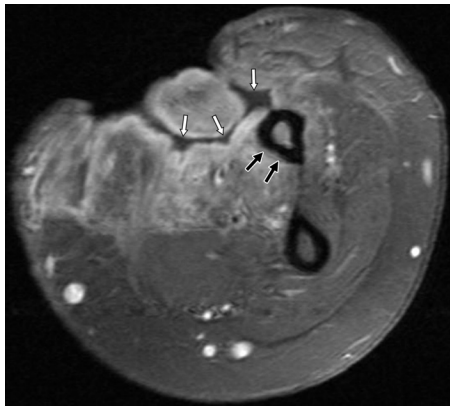

Figure 12. Pyomyositis related to skin ulceration in a 54-year-old man who was an injection drug user. Axial contrast material–enhanced fat-suppressed T1-weighted MR image of the left forearm shows deep skin ulceration of the volar forearm, with thin linear tracks of nonenhancing fluid tracking to the distal radius (white arrows), surrounded by high-signal-intensity enhancement of the exposed flexor musculature related to pyomyositis. Note the subtle increased marrow signal intensity and periostitis of the radius (black arrows), indicating early osteomyelitis.

against HMG-CoA reductase are identified in such patients. The exact mechanism of muscle damage may relate to this autoantibody, other soluble factors, aberrant drug processing, or infiltration by immune cells (29,30).

Antiretroviral drugs (eg, azidothymidine), corticosteroids, calcineurin inhibitors, vitamin metabolites, anabolic agents, and a host of other medications can also lead to myopathy (31). Azidothymidine myopathy develops in up to 6% of patients with HIV infection, related to drug interaction with mitochondrial DNA polymerase;

it differs from pyomyositis by being symmetric, without intramuscular fluid collections (32). Drug-induced muscle disease is a diagnosis of exclusion. A temporal link between symptoms and initiation of drug therapy, or improvement following tapering/cessation of the drug, suggests this diagnosis (33). Illicit agents, such as cocaine, can result in extensive myonecrosis related to arterial vasoconstriction or direct muscle toxicity; such patients may not disclose their drug use (34) (Fig 11).

HIV-related Myopathy

The pathophysiology of HIV-related myopathies is multifactorial, related to the virus, its components, and the host's altered immune response (35). Patients with HIV infection are at increased risk for infectious pyomyositis, drug-induced myopathy, and polymyositis (35–37). While the increased frequency of infection is well recognized in immunocompromised patients, noninfectious inflammatory polymyositis is actually more common than pyomyositis in patients with HIV infection, resulting in proximal muscle weakness and elevated creatine kinase levels. Inflammatory polymyositis may be the sole manifestation of HIV infection or appear years after clinically apparent immunodeficiency (36,37). Other less common HIV-related myopathies include rhabdomyolysis, necrotizing noninflammatory myopathy, nemaline rod myopathy, subclinical myopathy, and denervation caused by HIV-related peripheral neuropathy (36,38).

Muscle Infection/Pyomyositis

Pyomyositis, an acute bacterial infection of muscle, can occur by hematogenous dissemination, spread from adjacent osteomyelitis or septic arthritis, or direct inoculation through a soft-tissue defect (Fig 12). Infection risk is increased in muscle that is compromised by trauma, surgery, malnutrition, or ischemia (39–41). While originally considered a tropical disease of children and young adults, it is commonly associated with diabetes, intravenous drug use, and an immunocompromised state and can be multifocal or bilateral in up to 40% of such patients (2,41). *Staphylococcus aureus* is implicated in up to 90% of cases, but atypical and multiorganism infections do occur, particularly in immunocompromised patients (39,42). The thigh muscles are most commonly affected, particularly the quadriceps, followed by the gluteal and psoas muscles (40,41).

MR imaging demonstrates increased volume of the affected muscles on T1-weighted images; T2-weighted images show increased muscle signal intensity related to fluid and pus. Images obtained after the administration of contrast media often reveal small fluid collections related to myonecrosis or focal fluid accumulation. Large areas of
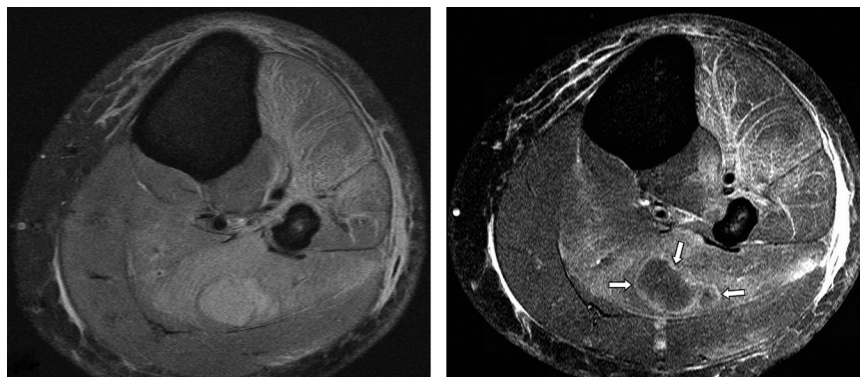
a.   b.

Figure 13. Calf abscess in a 30-year-old man with endocarditis of a bicuspid aortic valve, with septic emboli related to *S aureus* vegetations. **(a)** Axial fat-suppressed PD-weighted MR image shows pyomyositis of the anterior and deep posterior compartments of the lower leg, with an intramuscular abscess of the soleus muscle. **(b)** Axial contrast-enhanced fat-suppressed T1-weighted MR image shows a small area of nonenhancing fluid, with a thin rim of enhancement, compatible with an abscess (arrows). The patient underwent incision and drainage.

Figure 14. Disseminated muscle involvement related to cysticercosis in an adult man. Coronal fat-suppressed T2-weighted MR image of the posterior chest and abdomen shows innumerable subcentimeter hyperintense lesions, oriented parallel to the muscle fibers in all visible muscles. (Courtesy of Travinder Buxi, MD, Ganga Ram Hospital, Delhi, India.)
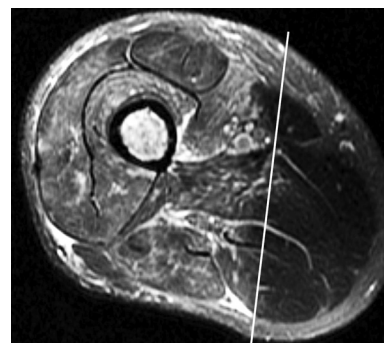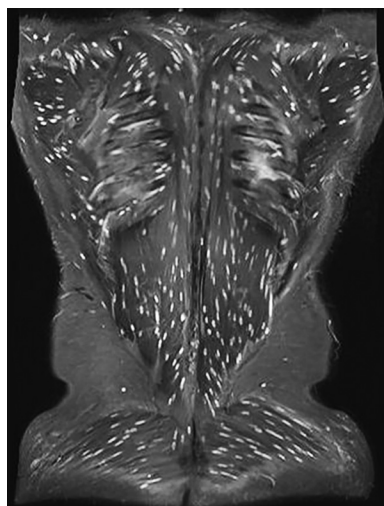

Figure 15. Radiation-induced myositis in a 34-year-old man who underwent treatment for metastatic disease to the right femur, related to a primary malignant nerve sheath tumor of the ipsilateral ankle. Axial STIR MR image of the right midthigh shows a sharp bandlike demarcation (white line) between the abnormal irradiated muscle (predominantly of the anterior right thigh) and the normal muscle more posteriorly. Note that the demarcation is independent of any normal compartment boundaries.

nonenhancement typically represent an abscess, the hallmark of pyomyositis (41) (Fig 13). Abscesses are usually hypointense or isointense on T1-weighted images and hyperintense on T2-weighted images. Intralesional gas may manifest. T1-weighted images may show a thin peripheral rim of increased signal intensity, referred to as the "penumbra sign" (35,42–44). There is typically extensive inflammation of the adjacent tissues, which helps distinguish an abscess from a soft-tissue tumor (41).

Cysticercosis

Cysticercosis is a parasitic infection that is caused by *Taenia solium* and is common in developing countries, where persons are infected by eating improperly cooked pork (45,46). The central nervous system is the most common site of symptomatic disease; when cysticercosis affects muscle, there is typically concomitant neural involvement (45,46). Muscle involvement by cysticercosis can be asymptomatic or manifest as myalgia, a solitary

mass, or, most commonly, multiple intramuscular cysts (46) (Fig 14). The appearance of intramuscular lesions varies as the disease progresses through its vesicular, colloid, granular-nodular, and calcific stages (47). The early stages, before calcification, are nonspecific, particularly when there is a solitary lesion (45,46). The late calcific stage is distinctive, showing multiple small ovoid calcifications oriented parallel to the muscle fibers.

Radiation Therapy

Radiation therapy results in muscle edema caused by radiation-induced myositis, as well as intermuscular septal edema related to radiation-induced vasculitis (48). Signal intensity alterations at MR
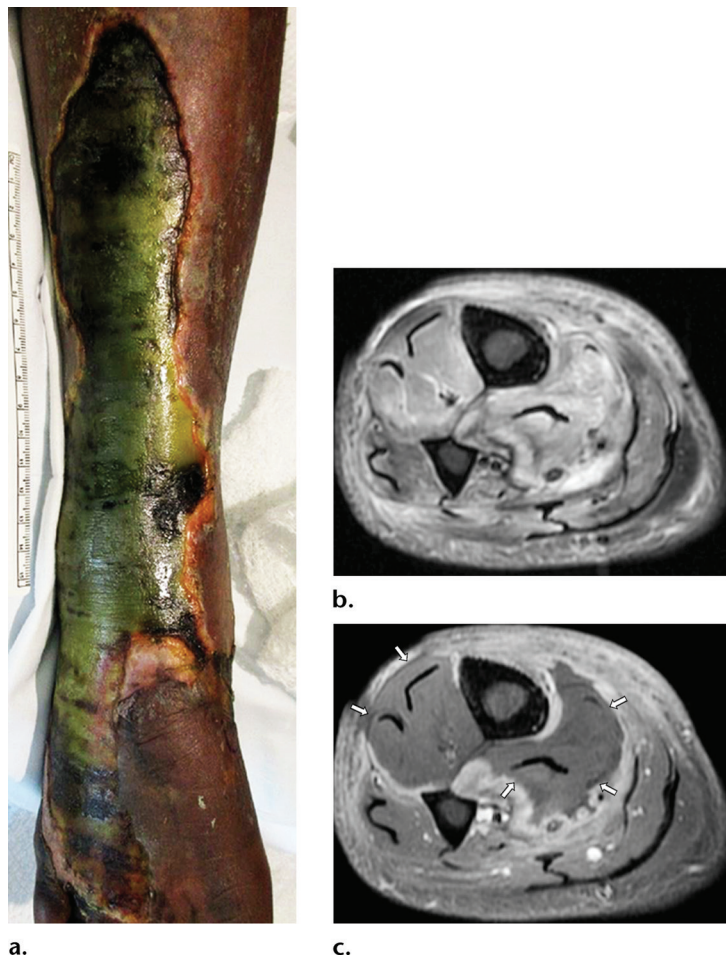
Figure 16. ACS of the right calf related to an ulcerative *Pseudomonas aeruginosa* infection in a 59-year-old woman with acute myelogenous leukemia. **(a)** Photograph of the right lower leg shows green discoloration of the tissues (ecthyma gangrenosum), characteristic of a *P aeruginosa* infection. **(b)** Axial fat-suppressed T2-weighted MR image of the right calf shows increased signal intensity in all of the musculature of the right lower leg. **(c)** Axial contrast-enhanced fat-suppressed T1-weighted MR image shows large areas of nonenhancement in the anterior and deep posterior compartments of the lower leg (arrows), indicating failure of perfusion. The patient required fasciotomy and extensive debridement.

imaging peak 6–12 months after therapy but may persist for years (9,48). Radiation-induced changes should be considered whenever there is a sharp bandlike demarcation between abnormal and normal muscle, particularly if this interface is within a single muscle (9,49) (Fig 15). Uncommonly, irradiated muscle can infarct, resulting in distorted enhancement and liquefaction. Rarely, irradiated muscle can exhibit a phenomenon known as radiation recall, whereby a drug, typically a chemotherapeutic agent, generates an acute inflammatory reaction at a prior site of radiation years after therapy (50). Over time, irradiated muscles can atrophy and undergo fibrosis.

Myonecrosis/Rhabdomyolysis
Myonecrosis refers to infarction of muscle, typically followed by tissue liquefaction. Rhabdomyolysis refers to myonecrosis complicated by myoglobinemia, which can lead to disseminated intravascular coagulation, acute renal failure, or even death (51,52). Muscle damage of sufficient severity from any cause can result in myonecrosis. Causes include compartment syndrome, diabetes, trauma, exercise, heatstroke, radiation, infection, metabolic disorders, seizures, envenomation,

toxins, and medicinal or illicit drug use (51,53). Clinical findings can be nonspecific, and muscle pain may not be a prominent feature. T1-weighted images show mild hyperintensity owing to hemorrhage or protein concentration, while T2-weighted images demonstrate patchy hyperintense signal owing to a combination of edema, necrosis, and hemorrhage. There are two appearances seen following contrast medium administration: type 1 demonstrates nonspecific homogeneous edema and enhancement, reflecting the initial stages of myonecrosis before liquefaction; whereas type 2 ("stipple" sign) shows inhomogeneity with foci with low signal intensity within demarcated regions of nonenhancement, representing either residual viable muscle or inflammatory vessels (54,55). However, the use of a contrast medium is precluded owing to acute renal failure in at least 13% of patients with rhabdomyolysis (51).

Acute Compartment Syndrome.—Elevated compartmental pressure related to trauma, compression, overexertion, infection, or neoplasm can cause abnormal pressure gradients between the vasculature and the muscle, resulting in ACS (2,56) (Fig 16). ACS most commonly affects the

Figure 17. ACS of the lateral compartment of the left lower leg in a 48-year-old woman with hereditary angioneurotic edema, resulting in repetitive episodes of compartment syndrome. **(a)** Axial fat-suppressed PD-weighted MR image shows marked swelling and diffuse increased signal intensity involving the peroneus longus and brevis muscles (arrows). **(b)** Frontal radiograph of the left lower leg obtained 2 years following the last acute episode shows calcification corresponding to the lateral compartment, indicating that the tissues have undergone myonecrosis. **(c)** Corresponding axial fat-suppressed PD-weighted MR image shows regression of muscle edema, with formation of a masslike area with low signal intensity and a hypointense periphery (arrows), representing peripheral calcifications, enclosing muscle that has undergone liquefactive necrosis, consistent with calcific myonecrosis.

Figure 18. Rhabdomyolysis in a 52-year-old woman with a history of poorly controlled diabetes who presented with acute right thigh pain. Axial T1-weighted **(a)** and contrast-enhanced fat-suppressed T1-weighted **(b)** MR images of the right thigh show a well-marginated area of nonenhancement related to muscle infarction (arrows) at the epicenter of the muscle inflammation. The slightly higher T1 signal intensity within the lesion is likely due to hemorrhage. This appearance is indistinguishable from a muscle abscess. The results of a needle aspiration confirmed rhabdomyolysis.
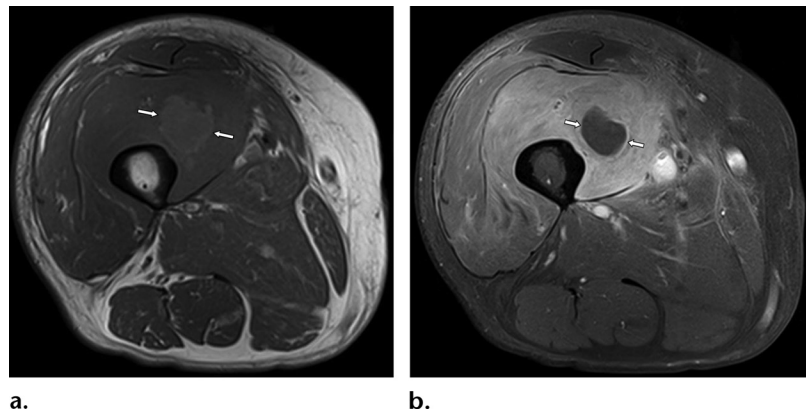
lower leg but also occurs in the thighs, forearms, and paraspinal musculature. ACS is diagnosed clinically, confirmed by intracompartmental pressure measurements, and requires prompt surgical decompression to prevent myonecrosis. Imaging plays a limited role in diagnosis when the clinical signs of arterial insufficiency (pain, paresthesia, pallor, and pulselessness) have already manifested (57). If MR imaging is performed because the diagnosis is not suspected, it demonstrates normal or increased signal intensity on T1-weighted images owing to hemorrhage and increased signal intensity on T2-weighted images owing to interstitial edema. Contrast-enhanced MR images best illustrate the perfusion failure within an affected compartment.

Chronic compartment syndrome may result in atrophy, fibrosis, calcification, or, rarely, masslike lesions referred to as calcific myo-

necrosis. Calcific myonecrosis is an unusual condition, typically affecting the calf, in which a chronic painless fusiform mass develops where liquefied necrotic muscle is surrounded by peripheral calcifications (58). MR imaging shows a heterogeneous mass on T2-weighted images, with a fluid-filled nonenhancing center following contrast medium administration (Fig 17). The peripheral calcifications are more apparent at radiography and CT.

Diabetic Rhabdomyolysis.—Myonecrosis/rhabdomyolysis is an uncommon complication of poorly controlled type 1 or 2 diabetes (52,59,60). Patients present with abrupt severe pain and swelling, typically at the anterior thigh or posterior calf muscles (59). Fever manifests in 10% of cases, making diabetic rhabdomyolysis difficult to distinguish clinically from infection. Diabetic
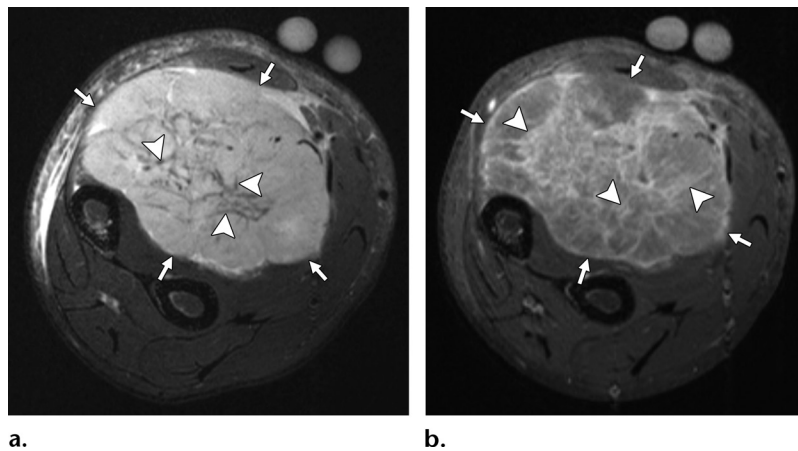
a.   **b.**

Figure 19. Primary rhabdomyosarcoma in an adolescent boy who presented with a rapidly enlarging forearm mass. **(a)** Axial fat-suppressed T2-weighted MR image shows a large mass with heterogeneous increased signal intensity (arrows) and internal septa (arrowheads) in the volar compartment of the forearm. The normal musculature is replaced with a mild amount of overlying subcutaneous edema. **(b)** Axial postcontrast fat-suppressed T1-weighted MR image shows inhomogeneous enhancement, with linear and septal bands (arrowheads) of high signal intensity dispersed throughout the lesion. The results of a percutaneous biopsy confirmed rhabdomyosarcoma.

rhabdomyolysis is frequently multifocal and bilateral, with up to 40% of patients showing alterations of multiple muscle compartments. At T1-weighted imaging, diabetic myonecrosis results in muscle enlargement, effacement of intramuscular fatty septa, and occasionally hemorrhagic necrosis; perifascial fluid and increased muscle signal intensity are seen on T2-weighted images.

At imaging after the administration of contrast media (postcontrast), the ischemic muscle contains patchy nonenhancing regions of necrotic muscle that can simulate abscess. While myonecrosis tends to not show thick rim enhancement or as much mass effect as would be expected for the amount of excess fluid within the affected muscles, it is difficult to distinguish from an abscess (Fig 18). Because there is considerable overlap in the imaging appearances of pyomyositis and diabetic myonecrosis, fluid aspiration is typically necessary to exclude infection (59,60).

Pattern 3: Muscle Mass

Intramuscular masses include malignant or benign primary neoplasms, metastatic disease, and nonneoplastic masslike lesions related to infection, trauma, inflammation, or other underlying disorders. The differential diagnosis of an intramuscular mass depends on the patient's age, pertinent clinical history, location of the mass, and its imaging appearance. A few intramuscular masses demonstrate unique MR imaging characteristics, allowing a specific diagnosis. It is beyond the scope of this article to discuss neoplasia in detail; only a few intramuscular masses are highlighted, emphasizing their characteristic imaging findings.

Malignant Primary Neoplasms of Muscle

The incidence of primary malignancy arising in muscle is surprisingly low given the large volume of this tissue in the body. The most common primary tumors arising in muscle are soft-tissue sarcomas of mesenchymal origin. While 12 000

new soft-tissue sarcomas are diagnosed annually in the United States (61), it should be noted that a substantial proportion arise in extramuscular tissues. In muscle, liposarcomas, neoplasms of fibrous origin, and lymphomas represent the most common primary malignancies. Less commonly, leiomyosarcomas, angiosarcomas, extraskeletal osteosarcomas (osseous), and synovial sarcomas develop in skeletal muscle (62). Intramuscular malignancies typically appear as heterogeneous infiltrative masses with variable degrees of enhancement and necrosis. Liposarcoma can be recognized if it contains macroscopic fat that is bright on T1-weighted images and suppresses with selective fat saturation. Tumors of fibrous origin may contain confluent regions of low signal intensity on T2-weighted images, but this finding is neither sensitive nor specific. In the majority of cases of skeletal malignancy, a biopsy is needed to establish a specific histologic diagnosis.

Malignant neoplasms derived from skeletal muscle cells and their precursors, known as rhabdomyosarcomas, are uncommon and account for less than 5% of all sarcomas (63,64). The majority of rhabdomyosarcomas are of the embryonal subtype and develop in children at extramuscular sites such as the head, neck, and genitourinary tract. The less common alveolar subtype affects all ages and typically arises in muscle, but overall, fewer than 25% of rhabdomyosarcomas arise within muscle (62). Adult rhabdomyosarcoma is rare, and the most common histologic subtype is anaplastic (also referred to as pleomorphic) (65). Rhabdomyosarcomas are nonspecific in appearance, resembling other soft-tissue sarcomas and often with central necrosis (Fig 19).

Skeletal muscle involvement is seen in 1%–2% of patients with lymphoma and typically results from muscle metastasis from systemic lymphoma or extension from the adjacent bone or lymph nodes (66). Primary extranodal lymphoma of
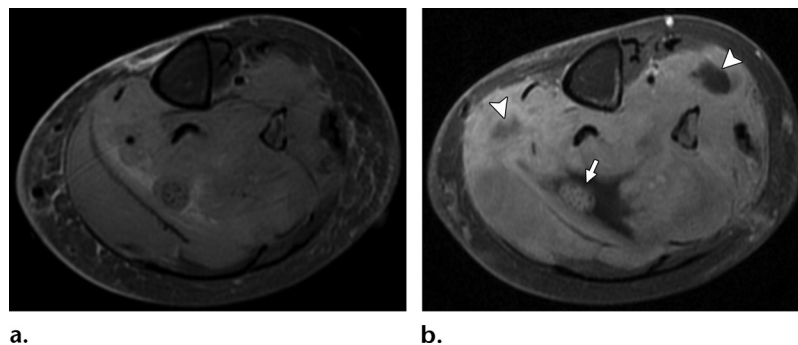
Figure 20. Lymphoma involving multiple muscle compartments in a 74-year-old woman. Axial fat-suppressed T2-weighted **(a)** and postcontrast fat-suppressed T1-weighted **(b)** MR images of the left calf show near-complete replacement of the normal musculature, with an intermediate-signal-intensity infiltrative tumor that enhances following contrast medium administration. A few areas of tumor necrosis are evident on the postcontrast image (arrowheads in **b**). Note the enlargement and infiltration of the tibial nerve (arrow in **b**), which also enhances.

Figure 21. Low-flow vascular malformation in a 35-year-old woman who presented with a mass along the ulnar aspect of the right elbow. **(a)** Coronal T1-weighted MR image shows a heterogeneous lesion (arrowheads) with low signal intensity and interspersed fat within. **(b)** Corresponding coronal fat-suppressed T2-weighted image shows nonuniform increased signal intensity, with low-signal-intensity bands corresponding to the fat striations within the mass (arrowheads). Note the small hypointense focus (arrow) at its deep aspect, which represents a phlebolith, typical of a low-flow vascular malformation.
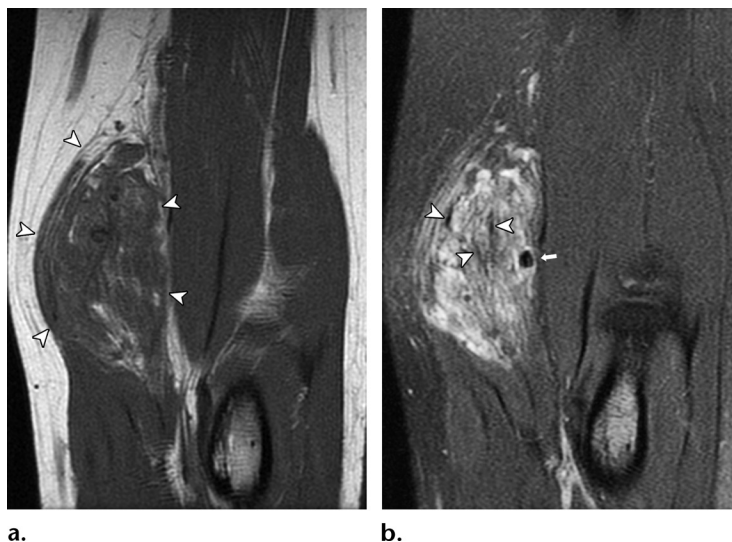
muscle is rare, typically affecting the thigh, trunk, upper arm, or calf in older patients, with an increased incidence in males and patients with HIV infection (67–69).

At MR imaging, muscle lymphoma most commonly manifests as an infiltrative mass, characteristically elongated along the course of the muscle fascicles, often with relative preservation of the intramuscular fat planes. It typically exhibits hyperintense signal on T1-weighted images and intermediate signal intensity on T2-weighted images, with diffuse enhancement or thick peripheral bandlike enhancement of the involved muscle (66,68,69). Involvement of multiple compartments is seen in up to 70% of patients. The presence of multiple masses, intralesional vessels, extension of tumor along neurovascular bundles, thick fascial enhancement, and adjacent subcutaneous infiltration is suggestive of lymphoma (66–69) (Fig 20). Less commonly,

lymphoma manifests as increased muscle signal intensity without a discrete mass, although the involved muscle tends to be enlarged and enhances in such cases.

Benign Primary Neoplasms of Muscle

The most common benign neoplasms arising within muscle are lipomas, hemangiomas/vascular malformations, myxomas, and fibromatoses (70). Lipomas are the most common soft-tissue neoplasm and can be classified as superficial or deep. Deep lipomas are commonly intramuscular but may also be intermuscular, typically affecting the large muscle groups in the extremities of adult men (71). Simple lipomas are isointense relative to fat on all pulse sequences. Large size, local symptoms, rapid growth, and nodular or thick (>2 mm) septal enhancement suggest an atypical lipomatous tumor or a well-differentiated liposarcoma (71).
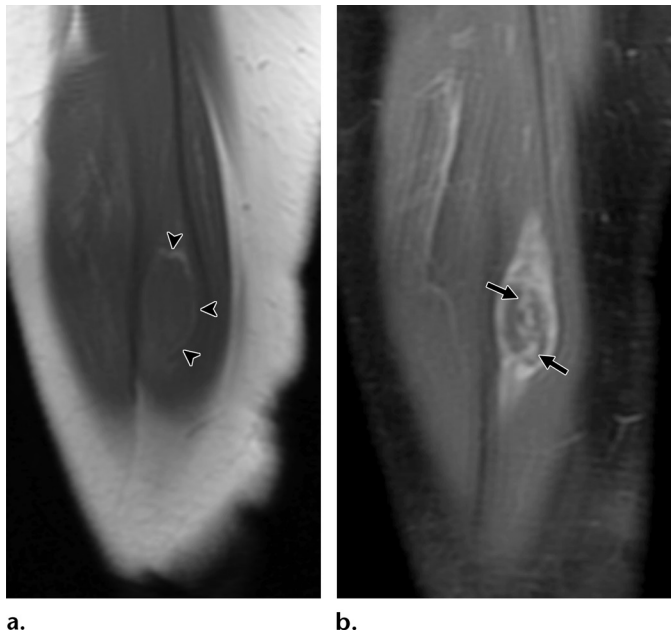
Figure 22. Intramuscular myxoma in a 46-year-old woman with a painless mass in the right thigh for 1 year. **(a)** Coronal T1-weighted MR image of the right midthigh shows a well-circumscribed homogeneous cystic-appearing mass with low signal intensity and a thin peripheral halo of fat (arrowheads) within the right rectus femoris muscle. **(b)** Coronal fat-suppressed T1-weighted MR image shows wall enhancement and regions of nodular enhancement with high signal intensity within the mass (arrows), indicating interspersed soft-tissue components. The findings exclude a diagnosis of uncomplicated simple cyst.
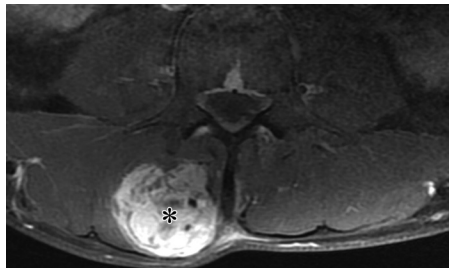

Figure 23. Metastasis in the right paraspinal musculature in a 31-year-old man with widespread metastatic disease from a primary lower extremity sarcoma. Axial postcontrast fat-suppressed T1-weighted image shows a large enhancing intramuscular mass, involving the right transversospinalis and erector spinae muscles (∗). Note the mass effect and displacement of the overlying fascia.

Hemangiomas and vascular malformations are common benign and dysplastic vascular epithelial lesions, respectively, which typically demonstrate a lobulated and septated appearance, markedly hyperintense T2-weighted signal intensity, and enhancement on postcontrast images (72). Phleboliths are common in low-flow malformations (Fig 21), whereas enlarged serpentine flow voids suggest high-flow malformations.

Intramuscular myxoma is a benign tumor of uncertain differentiation that histologically resembles the mucinous substance of the umbilical cord (73). It is typically well marginated and homogeneous and, thus, is easily mistaken for a ganglion or benign cyst. MR imaging features that distinguish myxoma from a cyst include a peripheral rind of fat, edema in the surrounding musculature, and, most importantly, internal enhancement on postcontrast images (73) (Fig 22).

The fibromatoses are a group of benign fibroblastic proliferations that show infiltrative growth and can be locally aggressive. These lesions are classified by location as superficial or deep. Deep lesions are further categorized by age, location, and the specific tissue deposited. Desmoid-type fibromatosis is usually intramuscular or intermuscular and most frequently manifests in women during the 2nd to 4th decades of life. Lesions may be well defined or infiltrative with fascial plane extension (74). The MR imaging appearance reflects the amount of collagen and cellularity in the lesion, with more collagenous-containing lesions demonstrating low T1 and T2 signal intensities (74).

Metastatic Disease

Although muscle is highly vascularized and comprises 50% of total body mass, skeletal muscle metastases are rare, with autopsy studies citing a 0.03%–17.5% prevalence (75). Muscle metastases are most commonly located in the abdominal wall or paravertebral musculature, related to lung carcinoma, melanoma, or primary malignancies of the genitourinary and gastrointestinal systems; the latter types presumably disseminate to muscle by the paravertebral vascular plexus (75,76) (Fig 23). Muscle metastases are typically asymptomatic; the majority are diagnosed incidentally during routine staging. Their most common imaging appearance, seen in over half of cases, is that of a discrete intramuscular mass. Metastases can also appear abscess-like, related to central necrosis; ill-defined owing to infiltration; calcified; or hemorrhagic, simulating posttraumatic bleeding (75).

Hematomas

Hematomas are commonly encountered intramuscular masses, typically resulting from trauma or anticoagulant therapy. Hematomas can lead to elevated compartment pressure, serve as a nidus for infection, or cause compressive neuropathy (40,55,77). At MR imaging, hematomas demonstrate variable signal intensity, depending on their stage of blood product degradation. A peripheral high-signal-intensity ring related to methemoglobin on T1-weighted images in the subacute stage is the most distinctive finding indicating a hematoma (Fig 24).

Organizing hematomas often appear irregular and heterogeneous and may show patchy internal enhancement that can be mistaken for malignancy. Hematomas typically show rim enhancement at postcontrast imaging, a finding that may also be seen in necrotic neoplasms. When there is no clear history of injury or anticoagulation therapy, or when an intramuscular mass shows thick rim enhancement or substantial internal enhancement, an underlying neoplasm as the source of bleeding should be considered (8,9). It is prudent to follow such lesions with US to resolution to exclude an underlying neoplasm.

Nodular Myositis

Focal nodular myositis is a rare inflammatory pseudotumor of skeletal muscle that manifests as a rapidly enlarging and painful mass (78). Initial reports favored a traumatic or ischemic cause, but subsequent series describe an association with systemic polymyositis, suggesting an autoimmune basis (78,79). Other reports describe an association with underlying malignancy, suggesting that focal nodular myositis is a paraneoplastic phenomenon (80).

Focal nodular myositis is typically limited to a single muscle, but involvement of multiple muscles, either in the same or adjacent compartments, has been described (79). MR imaging findings are nonspecific, demonstrating a variably enhancing mass with surrounding edema (Fig 25). Tissue sampling is necessary to establish the diagnosis.

Sarcoidosis

Sarcoidosis is a chronic systemic noncaseating granulomatous disease that affects muscle in two forms: a generalized myopathy related to microscopic infiltration, and a nodular form with multiple discrete intramuscular masses (81,82). The diffuse form is not well depicted at MR imaging and is best diagnosed with gallium 67 (^{67}Ga) scintigraphy.

The nodular form, present in 1.4% of patients with sarcoidosis, typically affects the lower extremities and is distinctive. The masses are ovoid or cordlike, oriented longitudinally along muscle
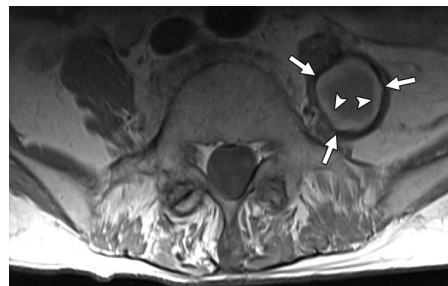

Figure 24. Psoas hematoma in a 73-year-old man treated with anticoagulants. Axial T1-weighted MR image of the lumbar spine shows a subacute hematoma (arrows) in the left psoas muscle. The hematoma shows intermediate signal intensity centrally that is slightly higher than that of the adjacent muscle. Note the thick rim with high signal intensity at the periphery of the lesion, related to methemoglobin formation at its margins (arrowheads).

fibers (81), often at the musculotendinous junction (82). Axial images reveal central spiculated hypointense signal related to hyalinized connective tissue from chronic inflammation, surrounded by hypercellular granulomas peripherally ("dark star" sign). In the longitudinal plane, this arrangement produces cordlike signal intensity alterations, with a hypointense inner stripe encased by hyperintense outer stripes ("three stripes" sign) (81) (Fig 26). Sarcoid nodules can resolve after steroid therapy and may be substituted by regions of atrophy and fatty replacement (82,83).

Postinjection Masses

Adverse reactions to illicit, therapeutic, cosmetic, or preventative inoculations can result in localized muscle infection, inflammation, and fibrosis. Injection-related fibrosis after intramuscular vaccinations resulting in cordlike contractures of the deltoid muscle is well described, causing muscle atrophy and fibrosis, skin dimpling, and secondary scapular winging (84). MR images show an elongated mass of low-signal-intensity fibrotic tissue, while radiographs may show soft-tissue calcifications (85) (Fig 27).

Aesthetic intramuscular injections can result in peculiar appearances related to inoculation of autologous fat, hyaluronic acid, or, most commonly, free silicone. Free silicone injections are widely used for buttock cosmesis, producing a distinctive starry sky–like appearance related to the innumerable round heterogeneous deposits within the gluteal muscles and subcutaneous tissues (86) (Fig 28).

Intramuscular Extension of Calcium Hydroxyapatite

Calcium hydroxyapatite most commonly involves the shoulder tendons. Tendinous deposits can extrude into nearby tissues, inciting an intense
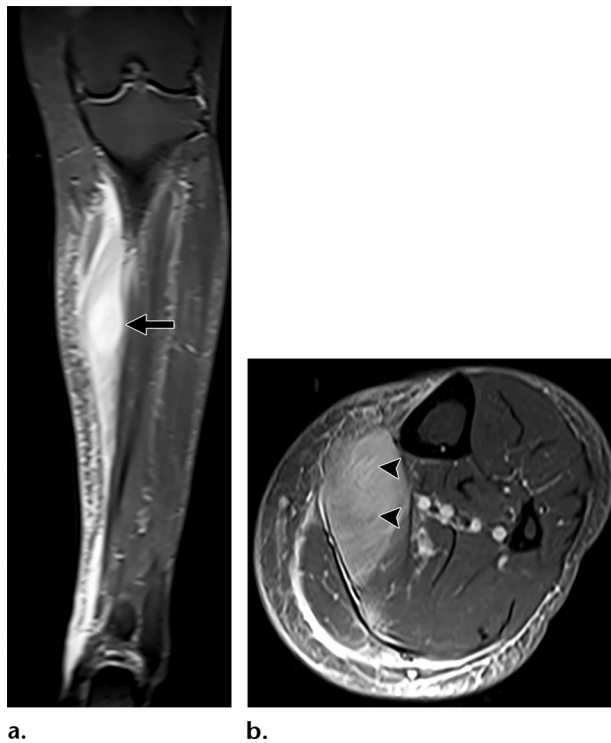
Figure 25. Focal nodular myositis in a 77-year-old woman with an enlarging calf mass after remote superficial lipoma resection. **(a)** Coronal fat-suppressed T2-weighted MR image of the lower leg shows a nearly homogeneous hyperintense mass (arrow) in the medial aspect of the soleus muscle with surrounding edema. **(b)** Axial fat-suppressed T2-weighted MR image shows subtle areas of hyperintense fibroblastic proliferation, interspersed between relatively hypointense muscle fascicles, creating a checkerboard-like pattern (arrowheads). Malignancy could not be excluded, so the patient was referred for biopsy. The results of the biopsy confirmed proliferative myositis, a type of nodular myositis.
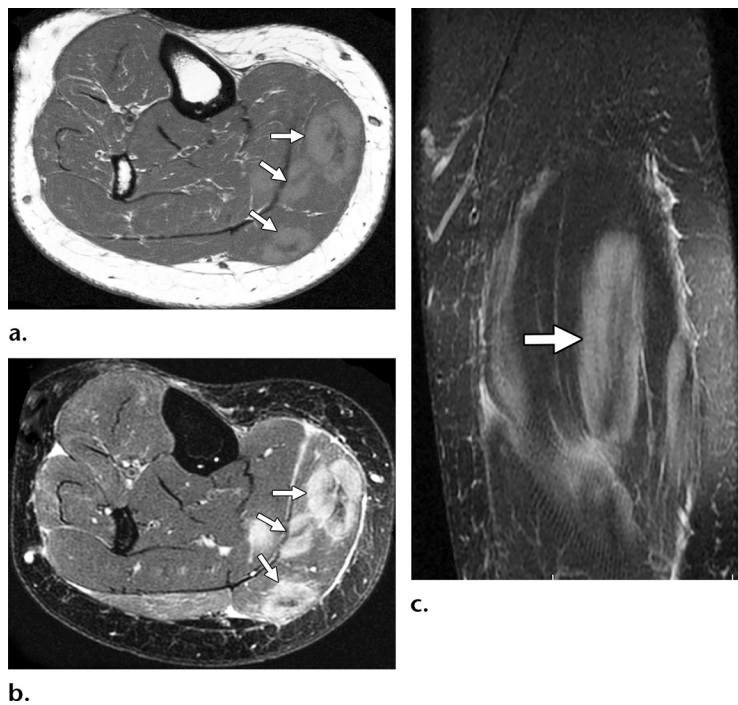
a.　　　　　　　b.

Figure 26. Nodular form of muscular sarcoidosis in a 64-year-old woman with tender lower leg masses. Axial T1-weighted **(a)**, axial fat-suppressed T2-weighted **(b)**, and coronal fat-suppressed T2-weighted **(c)** MR images of the right calf show intramuscular ovoid masses in the medial gastrocnemius (arrows) and soleus muscles. The central regions of hypointense signal reflect hyalinized connective tissue, while the thick rinds of increased peripheral signal intensity represent active granulomas, creating the "dark star" sign. These same findings, when viewed longitudinally on the coronal image **(c)**, create the "three-stripes" sign. (Courtesy of Anthony Peduto, MD, Westmead Hospital, Sydney, Australia.)

a.

b.

c.

inflammatory response, typically affecting the adjacent bursa. Intramuscular extension is uncommon, occurring most commonly at the supraspinatus and infraspinatus muscles, producing a small intramuscular mass with low signal intensity surrounded by a larger inflammatory response (87) (Fig 29). Intramuscular hydroxyapatite migration may be along the central myotendinous junction or deep to the epimysial muscle

covering. Radiographic correlation showing intramuscular extension of calcification confirms the diagnosis (87).

Pattern 4: Atrophy

Atrophy is characterized by loss of muscle tissue that manifests as decreased muscle size, often associated with fatty infiltration (88) (Fig 30). It is the irreversible end stage of numerous muscle
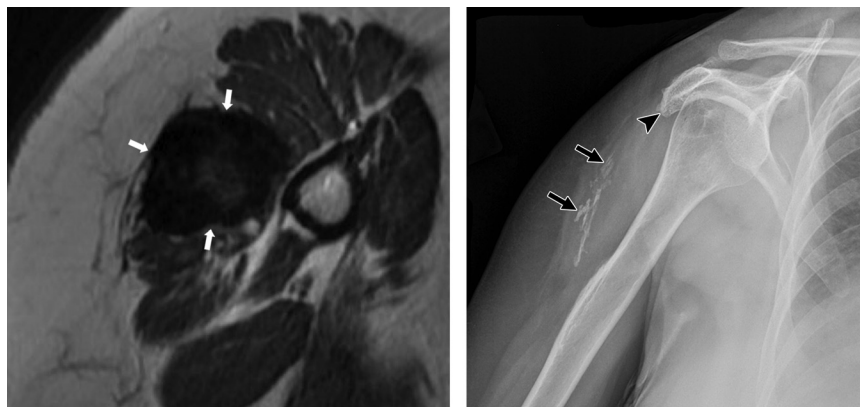
a.   b.

Figure 27. Fibrous contracture of the deltoid muscle in a 45-year-old woman who presented with a chronic right upper arm mass that developed after receiving an influenza vaccination. **(a)** Axial T2-weighted MR image of the right upper arm shows a mass with low signal intensity (arrows), compatible with fibrous tissue and calcification within the middle portion of the deltoid muscle. **(b)** Frontal radiograph shows a partially calcified mass (arrows) in the deltoid, which corresponds to the lesion seen at MR imaging. There is downsloping of the acromion (arrowhead) and suggestion of scapular winging related to the contractile nature of the lesion.

Figure 28. Nodules in a 63-year-old-woman with HIV infection who presented with bilateral hip pain and incidentally noted cosmetic silicone injections in both buttocks. Coronal fat-suppressed PD-weighted MR image of the posterior pelvis shows innumerable nodules within the subcutaneous fat and gluteus maximus muscles bilaterally. The nodules were isointense relative to muscle on T1-weighted images (not shown) and show slightly higher signal intensity than muscle (arrows), findings typical of free silicone injections.

diseases, including focal disorders such as trauma or denervation, as well as generalized disorders that are initially inflammatory. Atrophy is the principal finding in hereditary degenerative myopathies that produce disseminated muscle tissue loss without a prodromal inflammatory phase. Atrophy related to aging is referred to as *sarcopenia*, which is increasingly recognized as a substantial predictor of overall health. Atrophy is an important finding predicting loss of muscle power and function (89,90).

Congenital Myopathies
Muscular dystrophies are a heterogeneous group of progressive degenerative skeletal muscle disorders related to inherited gene defects (91). The best known are the Duchenne and Becker muscular dystrophies, inherited as X-linked recessive disorders, related to dystrophin gene dysfunction. Affected men present in childhood with pseudohypertrophy of the calf muscles and progressive lower extremity weakness. Maximal abnormalities are seen in the gluteal, thigh, and calf muscles bilaterally, with relative sparing of the adductor, gracilis, and sartorius muscles (91,92).

A host of other forms of muscular dystrophy have been characterized; almost all preferentially affect the lower extremities (91). A few forms, such as facioscapulohumeral muscular dystrophy, are

characterized by preferential involvement of the face, chest wall, trunk, and upper extremity musculature (92,93) (Fig 31). The diagnosis of muscular dystrophies is based on clinical examination, muscle enzymes measurements, genetic sequencing, and tissue sampling. MR imaging has been used primarily to identify disease distribution, monitor disease severity, and select optimal sites for biopsy (91,93–95). Quantitative techniques such as MR spectroscopy and T2 mapping show promise for earlier and more accurate assessment of muscle degeneration and fatty replacement in patients with muscular dystrophies (96,97).

Denervation Myopathy
Denervation myopathy refers to the physiologic and anatomic changes that occur when muscle
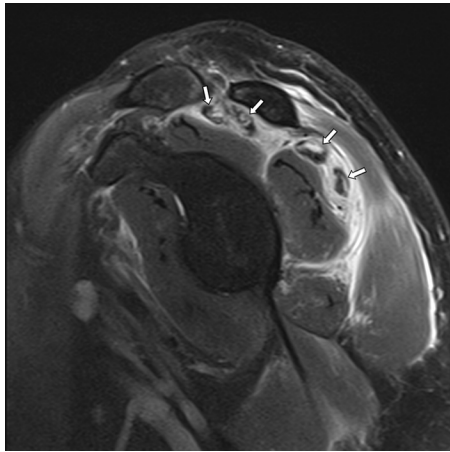
Figure 29. Intramuscular migration of calcium hydroxyapatite crystals in a 65-year-old woman with acute exacerbation of progressive left shoulder pain. Oblique sagittal fat-suppressed PD-weighted MR image of the left shoulder shows marked perifascial and intramuscular edema of the supraspinatus and infraspinatus muscles, related to intramuscular extension of the calcium hydroxyapatite (arrows). Calcifications were confirmed at radiography (not shown).
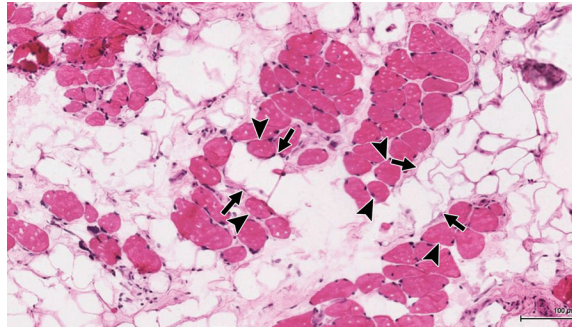

Figure 30. Fatty atrophy of supraspinatus muscle from a chronic rotator cuff tear in a patient undergoing reverse total shoulder arthroplasty. Photomicrograph of atrophic supraspinatus muscle specimen shows lobules of adipose tissue (arrows) interspersed between muscle fascicles (arrowheads), infiltrating and replacing the normal muscle tissue. Small foci of fat can also be seen within the degenerated fascicles. (Hematoxylin and eosin stain; original magnification, ×150.) (Courtesy of Samuel Ward, MD, University of California, San Diego, San Diego, Calif.)
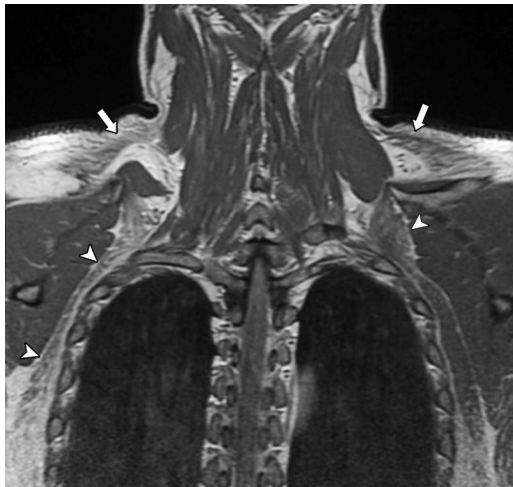

Figure 31. Facioscapulohumeral muscular dystrophy in a 35-year-old man with progressive arm weakness and loss of ability to whistle. Coronal T1-weighted MR image of the upper chest shows severe fatty atrophy of the trapezius (arrows) and serratus anterior (arrowheads) muscles bilaterally, characteristic of the preferential chest wall and shoulder girdle muscle involvement seen in this form of muscular dystrophy.

loses its innervation due to abnormalities of the central nervous system, spinal cord, peripheral motor nerve, or neuromuscular junctions at the muscle surface. Proposed mechanisms for denervation myopathy include capillary enlargement, increased vessel permeability, local metabolic effects, degeneration of muscle fibers, increased extracellular water, and proteolysis (98,99). MR imaging is sensitive for detecting muscle denervation and is a valuable adjunct to nerve conduc-

tion studies and electromyography for mapping the location and extent of disease, regardless of the underlying cause (100).

Denervation myopathy has variable appearances, depending on its duration. Acutely denervated muscle develops signal intensity alterations within 4 days of injury, preceding changes detected at electromyography (101). In acute denervation, T1-weighted images are normal, whereas fluid-sensitive images demonstrate uniformly increased muscle signal intensity (102,77). Unlike inflammatory disorders, there is no perimuscular fascial or subcutaneous fluid around the edematous muscle. In the subacute phase, signal intensity alterations persist on fluid-sensitive images, but T1-weighted images start to demonstrate atrophy (Fig 32). In chronic denervation, signal intensity alterations on fluid-sensitive images resolve, leaving a fat-replaced muscle that is irreversibly damaged (99).

The role of MR imaging in assessing denervation related to peripheral entrapment neuropathies has been emphasized in the musculoskeletal literature. Entrapment occurs in locations where a nerve courses through a fibro-osseous or fibromuscular tunnel, penetrates a muscle, or is impinged on by a mass (77,103). The key finding in peripheral nerve entrapment is that all affected muscles share a common innervation (Fig 33). The most common entrapment neuropathy relates to suprascapular nerve compression by a paralabral cyst arising from a glenoid labral tear. Cysts in the suprascapular fossa result in supraspinatus and infraspinatus denervation, whereas cysts located more distally in the spinoglenoid notch cause isolated infraspinatus denervation. Other common forms of entrapment neuropathy include compression of the peroneal nerve

Figure 32. Subacute denervation myopathy of the right calf related to idiopathic peripheral neuropathy in a 62-year-old man with lower leg pain and foot numbness. Electromyography showed evidence of chronic neurogenic changes in the muscles innervated by the tibial nerve. Axial T1-weighted **(a)** and fat-suppressed PD-weighted **(b)** MR images of the right calf show mild atrophy and diffusely increased abnormal signal intensity involving the superficial posterior compartment of the lower leg, as well as partial involvement of the deep posterior compartment.
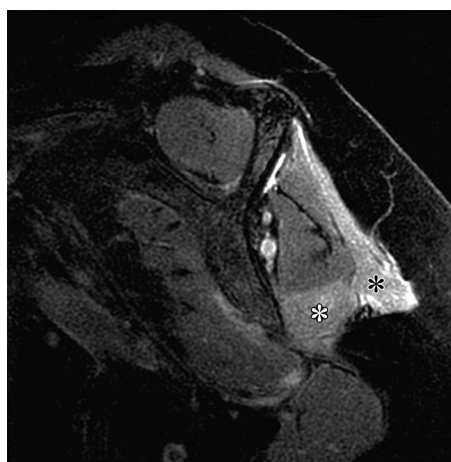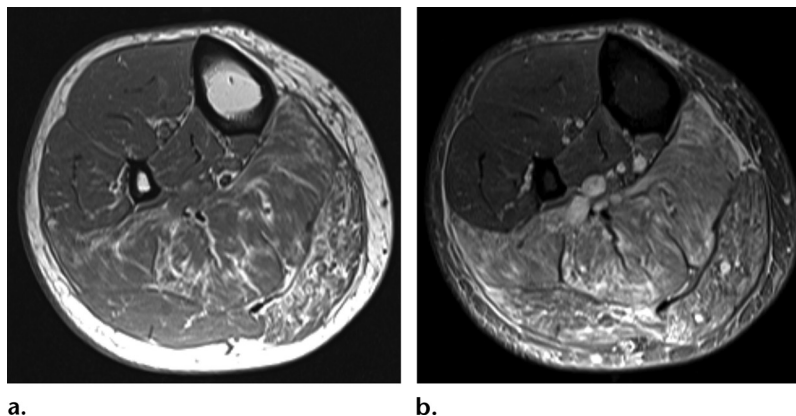
a.

b.

Figure 33. Subacute denervation myopathy 4 weeks after a stretching injury of the axillary nerve caused by glenohumeral dislocation in an adult woman. Sagittal fat-suppressed T2-weighted MR image of the right shoulder demonstrates diffuse denervation edema of the deltoid (black ∗) and teres minor (white ∗) muscles, findings indicative of axillary nerve injury.

Figure 34. Sarcopenia of the erector spinae muscles in a 58-year-old woman. Axial T1-weighted MR image at the L2 vertebral level demonstrates extensive symmetric fatty infiltration of the erector spinae muscles (arrowheads). Note the decreased volume of the psoas muscle bilaterally. Loss of muscle mass related to aging and low activity level is referred to as sarcopenia, which is increasingly recognized as an important risk factor for disability in older patients.

near the fibular neck, the posterior interosseous branch of the radial nerve at the anterior elbow, and the median nerve at the carpal tunnel (103).

Sarcopenia

Sarcopenia, also known as *myopenia* or *muscle wasting*, is defined as diminished muscle mass and function. Aging is an important risk factor; up to 50% of an adult's normal muscle mass can involute with advanced age, which has profound consequences on muscle function and physical health. Although aging is associated with muscle loss, the cause of sarcopenia is multifactorial and is also related to poor nutrition, inactivity, neurologic decline, hormonal alterations, and chronic disease (104). Sarcopenia has been associated with a number of adverse health outcomes such as prolonged disability, higher rates of hospital readmission and prolonged hospital stays, postoperative complications,

and increased mortality (105). Sarcopenia appears to be an independent predictor of adverse outcomes beyond other comorbidities that may manifest (106).

Histologic analysis reveals diminished quantity and quality of muscle fibers, particularly of the type II fiber fraction; fatty infiltration; and quiescence of satellite cells involved in muscle regeneration (104). CT of the abdomen/pelvis is frequently used to opportunistically assess paraspinal and truncal muscle volume as it is widely available and has been shown to be a valid measure of sarcopenia (106). Routine MR imaging sequences demonstrate volume loss and fatty infiltration; more sophisticated analysis of muscle composition can be obtained by using quantitative techniques such as fat-water imaging, lipid-suppressed mapping, diffusion-tensor imaging, and lipid spectroscopy (105) (Fig 34).

Conclusion

The MR imaging appearance of atraumatic muscle conditions can be classified into four broad patterns: *(a)* abnormal anatomy with normal signal intensity, *(b)* edema/inflammation, *(c)* intramuscular mass, and *(d)* atrophy. These four patterns may be seen in isolation or in combination, depending on the underlying disease and its severity and duration. An understanding of the disorders leading to each of these imaging patterns, coupled with clinical information, will help radiologists formulate appropriate differential considerations, suggest a specific diagnosis, plan biopsy, and guide appropriate management.

References

1. Costa AF, Di Primio GA, Schweitzer ME. Magnetic resonance imaging of muscle disease: a pattern-based approach. Muscle Nerve 2012;46(4):465–481.
2. McMahon CJ, Wu JS, Eisenberg RL. Muscle edema. AJR Am J Roentgenol 2010;194(4):W284–W292.
3. Carlier PG, Marty B, Scheidegger O, et al. Skeletal muscle quantitative nuclear magnetic resonance imaging and spectroscopy as an outcome measure for clinical trials. J Neuromuscul Dis 2016;3(1):1–28.
4. Pipitone N. Value of MRI in diagnostics and evaluation of myositis. Curr Opin Rheumatol 2016;28(6):625–630.
5. Elessawy SS, Borg MA, Mohamed MA, Elhewary GE, El-Salam EM. The role of MRI in the evaluation of muscle diseases. Egypt J Radiol Nucl Med 2013;44(3):607–615.
6. Kim HK, Laor T, Horn PS, Racadio JM, Wong B, Dardzinski BJ. T2 mapping in Duchenne muscular dystrophy: distribution of disease activity and correlation with clinical assessments. Radiology 2010;255(3):899–908.
7. Johnston JH, Kim HK, Merrow AC, et al. Quantitative skeletal muscle MRI: part 1—derived T2 fat map in differentiation between boys with Duchenne muscular dystrophy and healthy boys. AJR Am J Roentgenol 2015;205(2):W207–W215.
8. Kumar Y, Wadhwa V, Phillips L, Pezeshk P, Chhabra A. MR imaging of skeletal muscle signal alterations: systematic approach to evaluation. Eur J Radiol 2016;85(5):922–935.
9. May DA, Disler DG, Jones EA, Balkissoon AA, Manaster BJ. Abnormal signal intensity in skeletal muscle at MR imaging: patterns, pearls, and pitfalls. RadioGraphics 2000;20(Spec No):S295–S315.
10. Boutin RD, Pathria MN. Magnetic resonance imaging of muscle. In: Hodler J, von Schulthess GK, Zollikofer CL, eds. Musculoskeletal diseases 2013-2016. Milan, Italy: Springer-Verlag, 2013; 161–170.
11. Sookur PA, Naraghi AM, Bleakney RR, Jalan R, Chan O, White LM. Accessory muscles: anatomy, symptoms, and radiologic evaluation. RadioGraphics 2008;28(2):481–499.
12. Brodie JT, Dormans JP, Gregg JR, Davidson RS. Accessory soleus muscle: a report of 4 cases and review of literature. Clin Orthop Relat Res 1997;337(337):180–186.
13. Timins ME. Muscular anatomic variants of the wrist and hand: findings on MR imaging. AJR Am J Roentgenol 1999;172(5):1397–1401.
14. Christodoulou A, Terzidis I, Natsis K, Gigis I, Pournaras J. Soleus accessorius, an anomalous muscle in a young athlete: case report and analysis of the literature. Br J Sports Med 2004;38(6):e38.
15. Cheung Y. Normal variants: accessory muscles about the ankle. Magn Reson Imaging Clin N Am 2017;25(1):11–26.
16. Herzog RJ. Accessory plantaris muscle: anatomy and prevalence. HSS J 2011;7(1):52–56.
17. Theodorou DJ, Theodorou SJ, Kakitsubata Y. Skeletal muscle disease: patterns of MRI appearances. Br J Radiol 2012;85(1020):e1298–e1308.
18. Malik A, Hayat G, Kalia JS, Guzman MA. Idiopathic inflammatory myopathies: clinical approach and management. Front Neurol 2016;7(64):64.
19. Miller FW. Classification of idiopathic inflammatory myopathies. In: Kagen LJ, ed. The inflammatory myopathies. New York, NY: Humana, 2009; 15–28.
20. Bohan A, Peter JB, Bowman RL, Pearson CM. Computer-assisted analysis of 153 patients with polymyositis and dermatomyositis. Medicine (Baltimore) 1977;56(4):255–286.
21. O'Connell MJ, Powell T, Brennan D, Lynch T, McCarthy CJ, Eustace SJ. Whole-body MR imaging in the diagnosis of polymyositis. AJR Am J Roentgenol 2002;179(4):967–971.
22. Adams EM, Chow CK, Premkumar A, Plotz PH. The idiopathic inflammatory myopathies: spectrum of MR imaging findings. RadioGraphics 1995;15(3):563–574.
23. Yazici Y, Kagen LJ. The association of malignancy with myositis. Curr Opin Rheumatol 2000;12(6):498–500.
24. Schulze M, Kötter I, Ernemann U, et al. MRI findings in inflammatory muscle diseases and their noninflammatory mimics. AJR Am J Roentgenol 2009;192(6):1708–1716.
25. Paik JJ. Myopathy in scleroderma and in other connective tissue diseases. Curr Opin Rheumatol 2016;28(6):631–635.
26. Jung M, Bonner A, Hudson M, Baron M, Pope JE; Canadian Scleroderma Research Group (CSRG). Myopathy is a poor prognostic feature in systemic sclerosis: results from the Canadian Scleroderma Research Group (CSRG) cohort. Scand J Rheumatol 2014;43(3):217–220.
27. Schanz S, Henes J, Ulmer A, et al. Magnetic resonance imaging findings in patients with systemic sclerosis and musculoskeletal symptoms. Eur Radiol 2013;23(1):212–221.
28. Peters SA, Kley R, Tegenthoff M, Vorgerd M, Nicolas V, Heyer CM. MRI in lipid-lowering agent-associated myopathy: a retrospective review of 21 cases. AJR Am J Roentgenol 2010;194(4):W323–W328.
29. Mohassel P, Mammen AL. The spectrum of statin myopathy. Curr Opin Rheumatol 2013;25(6):747–752.
30. Mammen AL. Statin-associated autoimmune myopathy. N Engl J Med 2016;374(7):664–669.
31. Valiyil R, Christopher-Stine L. Drug-related myopathies of which the clinician should be aware. Curr Rheumatol Rep 2010;12(3):213–220.
32. Rodriguez W. Musculoskeletal manifestations of HIV disease. AIDS Clin Care 1998;10(7):49–51, 56.
33. Sidhu HS, Venkatanarasimha N, Bhatnagar G, Vardhanabhuti V, Fox BM, Suresh SP. Imaging features of therapeutic drug-induced musculoskeletal abnormalities. RadioGraphics 2012;32(1):105–127.
34. Roth D, Alarcón FJ, Fernandez JA, Preston RA, Bourgoignie JJ. Acute rhabdomyolysis associated with cocaine intoxication. N Engl J Med 1988;319(11):673–677.
35. Steinbach LS, Tehranzadeh J, Fleckenstein JL, Vanarthos WJ, Pais MJ. Human immunodeficiency virus infection: musculoskeletal manifestations. Radiology 1993;186(3):833–838.
36. Restrepo CS, Lemos DF, Gordillo H, et al. Imaging findings in musculoskeletal complications of AIDS. RadioGraphics 2004;24(4):1029–1049.
37. Wyatt SH, Fishman EK. CT/MRI of musculoskeletal complications of AIDS. Skeletal Radiol 1995;24(7):481–488.
38. Tehranzadeh J, O'Malley P, Rafii M. The spectrum of osteoarticular and soft tissue changes in patients with human immunodeficiency virus (HIV) infection. Crit Rev Diagn Imaging 1996;37(4):305–347.
39. Crum-Cianflone NF. Infection and musculoskeletal conditions: infectious myositis. Best Pract Res Clin Rheumatol 2006;20(6):1083–1097.
40. Fayad LM, Carrino JA, Fishman EK. Musculoskeletal infection: role of CT in the emergency department. RadioGraphics 2007;27(6):1723–1736.
41. Hayeri MR, Ziai P, Shehata ML, Teytelboym OM, Huang BK. Soft-tissue infections and their imaging mimics: from cellulitis to necrotizing fasciitis. RadioGraphics 2016;36(6):1888–1910.
42. Gordon BA, Martinez S, Collins AJ. Pyomyositis: characteristics at CT and MR imaging. Radiology 1995;197(1):279–286.
43. Fleckenstein JL, Burns DK, Murphy FK, Jayson HT, Bonte FJ. Differential diagnosis of bacterial myositis in AIDS: evaluation with MR imaging. Radiology 1991;179(3):653–658.

44. McGuinness B, Wilson N, Doyle AJ. The "penumbra sign" on T1-weighted MRI for differentiating musculoskeletal infection from tumour. Skeletal Radiol 2007;36(5):417–421.

45. Jankharia BG, Chavhan GB, Krishnan P, Jankharia B. MRI and ultrasound in solitary muscular and soft tissue cysticercosis. Skeletal Radiol 2005;34(11):722–726.

46. Mishra P, Pandey D, Tripathi BN. Cysticercosis of soleus muscle presenting as isolated calf pain. J Clin Orthop Trauma 2015;6(1):39–41.

47. White AC Jr. Neurocysticercosis: updates on epidemiology, pathogenesis, diagnosis, and management. Annu Rev Med 2000;51(1):187–206.

48. Richardson ML, Zink-Brody GC, Patten RM, Koh WJ, Conrad EU. MR characterization of post-irradiation soft tissue edema. Skeletal Radiol 1996;25(6):537–543.

49. Mulcahy H, Chew FS. MRI of nontumorous skeletal muscle disease: case-based review. AJR Am J Roentgenol 2011;196(6 suppl):S77–S85.

50. Delavan JA, Chino JP, Vinson EN. Gemcitabine-induced radiation recall myositis. Skeletal Radiol 2015;44(3):451–455.

51. Cervellin G, Comelli I, Lippi G. Rhabdomyolysis: historical background, clinical, diagnostic and therapeutic features. Clin Chem Lab Med 2010;48(6):749–756.

52. Sani MA, Campana-Salort E, Begu-LeCorroller A, Baccou M, Valéro R, Vialettes B. Non-traumatic rhabdomyolysis and diabetes. Diabetes Metab 2011;37(3):262–264.

53. Keltz E, Khan FY, Mann G. Rhabdomyolysis: the role of diagnostic and prognostic factors. Muscles Ligaments Tendons J 2014;3(4):303–312.

54. Lu CH, Tsang YM, Yu CW, Wu MZ, Hsu CY, Shih TT. Rhabdomyolysis: magnetic resonance imaging and computed tomography findings. J Comput Assist Tomogr 2007;31(3):368–374.

55. Cunningham J, Sharma R, Kirzner A, et al. Acute myonecrosis on MRI: etiologies in an oncological cohort and assessment of interobserver variability. Skeletal Radiol 2016;45(8):1069–1078.

56. Aweid O, Del Buono A, Malliaras P, et al. Systematic review and recommendations for intracompartmental pressure monitoring in diagnosing chronic exertional compartment syndrome of the leg. Clin J Sport Med 2012;22(4):356–370.

57. Weng KH, Tzeng WS, Shu GH, Chen CK. Magnetic resonance imaging of compartment syndrome: report of three cases. J Radiol Sci 2013;38(2):65–70.

58. O'Dwyer HM, Al-Nakshabandi NA, Al-Muzahmi K, Ryan A, O'Connell JX, Munk PL. Calcific myonecrosis: keys to recognition and management. AJR Am J Roentgenol 2006;187(1):W67–W76.

59. Huang BK, Monu JU, Doumanian J. Diabetic myopathy: MRI patterns and current trends. AJR Am J Roentgenol 2010;195(1):198–204.

60. Jelinek JS, Murphey MD, Aboulafia AJ, Dussault RG, Kaplan PA, Snearly WN. Muscle infarction in patients with diabetes mellitus: MR imaging findings. Radiology 1999;211(1):241–247.

61. American Cancer Society. Cancer facts and figures: 2017. https://www.cancer.org/content/dam/cancer-org/research/cancer-facts-and-statistics/annual-cancer-facts-and-figures/2017/cancer-facts-and-figures-2017.pdf. Published 2017. Accessed September 10, 2017.

62. Agamanolis DP, Dasu S, Krill CE Jr. Tumors of skeletal muscle. Hum Pathol 1986;17(8):778–795.

63. Weiss SW, Goldblum JR, Enzinger FM. Rhabdomyosarcoma. In: Enzinger and Weiss's soft tissue tumors. 4th ed. St Louis, Mo: Mosby, 2001; 771.

64. Kransdorf MJ. Malignant soft-tissue tumors in a large referral population: distribution of diagnoses by age, sex, and location. AJR Am J Roentgenol 1995;164(1):129–134.

65. Allen SD, Moskovic EC, Fisher C, Thomas JM. Adult rhabdomyosarcoma: cross-sectional imaging findings including histopathologic correlation. AJR Am J Roentgenol 2007;189(2):371–377.

66. Lim CY, Ong KO. Imaging of musculoskeletal lymphoma. Cancer Imaging 2013;13(4):448–457.

67. Beggs I. Primary muscle lymphoma. Clin Radiol 1997;52(3):203–212.

68. Suresh S, Saifuddin A, O'Donnell P. Lymphoma presenting as a musculoskeletal soft tissue mass: MRI findings in 24 cases. Eur Radiol 2008;18(11):2628–2634.

69. Chun CW, Jee WH, Park HJ, et al. MRI features of skeletal muscle lymphoma. AJR Am J Roentgenol 2010;195(6):1355–1360.

70. Wu JS, Hochman MG. Soft-tissue tumors and tumor-like lesions: a systematic imaging approach. Radiology 2009;253(2):297–316.

71. Murphey MD, Vidal JA, Fanburg-Smith JC, Gajewski DA. Imaging of synovial chondromatosis with radiologic-pathologic correlation. RadioGraphics 2007;27(5):1465–1488.

72. Teo EL, Strouse PJ, Hernandez RJ. MR imaging differentiation of soft-tissue hemangiomas from malignant soft-tissue masses. AJR Am J Roentgenol 2000;174(6):1623–1628.

73. Bancroft LW, Kransdorf MJ, Menke DM, O'Connor MI, Foster WC. Intramuscular myxoma: characteristic MR imaging features. AJR Am J Roentgenol 2002;178(5):1255–1259.

74. Murphey MD, Ruble CM, Tyszko SM, Zbojniewicz AM, Potter BK, Miettinen M. Musculoskeletal fibromatoses: radiologic-pathologic correlation. RadioGraphics 2009;29(7):2143–2173.

75. Surov A, Hainz M, Holzhausen HJ, et al. Skeletal muscle metastases: primary tumours, prevalence, and radiological features. Eur Radiol 2010;20(3):649–658.

76. Plaza JA, Perez-Montiel D, Mayerson J, Morrison C, Suster S. Metastases to soft tissue: a review of 118 cases over a 30-year period. Cancer 2008;112(1):193–203.

77. Kim SJ, Hong SH, Jun WS, et al. MR imaging mapping of skeletal muscle denervation in entrapment and compressive neuropathies. RadioGraphics 2011;31(2):319–332.

78. Flaisler F, Blin D, Asencio G, Lopez FM, Combe B. Focal myositis: a localized form of polymyositis? J Rheumatol 1993;20(8):1414–1416.

79. Gaeta M, Mazziotti S, Minutoli F, et al. MR imaging findings of focal myositis: a pseudotumour that may mimic muscle neoplasm. Skeletal Radiol 2009;38(6):571–578.

80. Naschitz JE, Yeshurun D, Dreyfuss U, Best LA, Misselevich I, Boss JH. Localized nodular myositis: a paraneoplastic phenomenon. Clin Rheumatol 1992;11(3):427–431.

81. Otake S. Sarcoidosis involving skeletal muscle: imaging findings and relative value of imaging procedures. AJR Am J Roentgenol 1994;162(2):369–375.

82. Moore SL, Teirstein AE. Musculoskeletal sarcoidosis: spectrum of appearances at MR imaging. RadioGraphics 2003;23(6):1389–1399.

83. Otake S, Imagumbai N, Suzuki M, Ohba S. MR imaging of muscular sarcoidosis after steroid therapy. Eur Radiol 1998;8(9):1651–1653.

84. Huang CC, Ko SF, Ko JY, et al. Contracture of the deltoid muscle: sonographic evaluation with MRI correlation. AJR Am J Roentgenol 2005;185(2):364–370.

85. Chen CK, Yeh L, Chen CT, Pan HB, Yang CF, Resnick D. Contracture of the deltoid muscle: imaging findings in 17 patients. AJR Am J Roentgenol 1998;170(2):449–453.

86. Frank SJ, Flusberg M, Friedman S, Sternschein M, Wolf EL, Stein MW. Aesthetic surgery of the buttocks: imaging appearance. Skeletal Radiol 2014;43(2):133–139.

87. Pereira BP, Chang EY, Resnick DL, Pathria MN. Intramuscular migration of calcium hydroxyapatite crystal deposits involving the rotator cuff tendons of the shoulder: report of 11 patients. Skeletal Radiol 2016;45(1):97–103.

88. Barry JJ, Lansdown DA, Cheung S, Feeley BT, Ma CB. The relationship between tear severity, fatty infiltration, and muscle atrophy in the supraspinatus. J Shoulder Elbow Surg 2013;22(1):18–25.

89. Gladstone JN, Bishop JY, Lo IK, Flatow EL. Fatty infiltration and atrophy of the rotator cuff do not improve after rotator cuff repair and correlate with poor functional outcome. Am J Sports Med 2007;35(5):719–728.

90. Boutin RD, Fritz RC. MRI of musculotendinous injuries: what's new?—part II: strain injuries. Curr Radiol Rep 2015;3:27.

91. Díaz-Manera J, Llauger J, Gallardo E, Illa I. Muscle MRI in muscular dystrophies. Acta Myol 2015;34(2-3):95–108.

92. Leung DG. Magnetic resonance imaging patterns of muscle involvement in genetic muscle diseases: a systematic review. J Neurol 2017;264(7):1320–1333.

93. Gerevini S, Scarlato M, Maggi L, et al. Muscle MRI findings in facioscapulohumeral muscular dystrophy. Eur Radiol 2016;26(3):693–705.

94. Liu GC, Jong YJ, Chiang CH, Jaw TS. Duchenne muscular dystrophy: MR grading system with functional correlation. Radiology 1993;186(2):475–480.

95. Leung DG, Carrino JA, Wagner KR, Jacobs MA. Whole-body magnetic resonance imaging evaluation of facioscapulohumeral muscular dystrophy. Muscle Nerve 2015;52(4):512–520.

96. Srivastava NK, Yadav R, Mukherjee S, Pal L, Sinha N. Abnormal lipid metabolism in skeletal muscle tissue of patients with muscular dystrophy: in vitro, high-resolution NMR spectroscopy based observation in early phase of the disease. Magn Reson Imaging 2017;38:163–173.

97. Kim HK, Serai S, Lindquist D, et al. Quantitative skeletal muscle MRI: part 2, MR spectroscopy and T2 relaxation time mapping-comparison between boys with Duchenne muscular dystrophy and healthy boys. AJR Am J Roentgenol 2015;205(2):W216–W223.

98. Kikuchi Y, Nakamura T, Takayama S, Horiuchi Y, Toyama Y. MR imaging in the diagnosis of denervated and reinnervated skeletal muscles: experimental study in rats. Radiology 2003;229(3):861–867.

99. Fleckenstein JL, Watumull D, Conner KE, et al. Denervated human skeletal muscle: MR imaging evaluation. Radiology 1993;187(1):213–218.

100. Wessig C, Koltzenburg M, Reiners K, Solymosi L, Bendszus M. Muscle magnetic resonance imaging of denervation and reinnervation: correlation with electrophysiology and histology. Exp Neurol 2004;185(2):254–261.

101. West GA, Haynor DR, Goodkin R, et al. Magnetic resonance imaging signal changes in denervated muscles after peripheral nerve injury. Neurosurgery 1994;35(6):1077–1085; discussion 1085–1086.

102. Kamath S, Venkatanarasimha N, Walsh MA, Hughes PM. MRI appearance of muscle denervation. Skeletal Radiol 2008;37(5):397–404.

103. Dong Q, Jacobson JA, Jamadar DA, et al. Entrapment neuropathies in the upper and lower limbs: anatomy and MRI features. Radiol Res Pract 2012;2012:230679.

104. Walston JD. Sarcopenia in older adults. Curr Opin Rheumatol 2012;24(6):623–627.

105. Boutin RD, Yao L, Canter RJ, Lenchik L. Sarcopenia: current concepts and imaging implications. AJR Am J Roentgenol 2015;205(3):W255–W266.

106. Boutin RD, Bamrungchart S, Bateni CP, et al. CT of patients with hip fracture: muscle size and attenuation help Predict Mortality. AJR Am J Roentgenol 2017;208(6):W208–W215.